Accepted Manuscript

Geological Society, London, Memoirs

Marie Byrd Land lithospheric mantle: A review of the xenolith record.

Monica R. Handler, Richard J. Wysoczanski & John A. Gamble

DOI: https://doi.org/10.1144/M56-2020-17

To access the most recent version of this article, please click the DOI URL in the line above. When citing this article please include the above DOI.

Received 17 June 2020
Revised 28 November 2020
Accepted 30 November 2020

Supplementary material at https://doi.org/10.6084/m9.figshare.c.5309814

Marie Byrd Land lithospheric mantle: A review of the xenolith record.

Monica R. Handler[1*], Richard J. Wysoczanski[2] & John A. Gamble[1]

[1] *School of Geography, Environment & Earth Science, Te Herenga Waka–Victoria University of Wellington, New Zealand*

[2] *National Institute of Water & Atmospheric Research, Private Bag 14901, Wellington, New Zealand*

**Corresponding author (email: monica.handler@vuw.ac.nz)*

Abstract: The Marie Byrd Land (MBL) lithospheric mantle xenolith record comprises over 100 samples from a range of localities spanning both major crustal terranes that comprise MBL: Ross and Amundsen provinces. Coarse granular to porphyroclastic in texture, the xenoliths are predominantly Type I spinel-bearing lherzolites to harburgites, but include rare dunite and pyroxenite examples. Garnet is absent and no hydrous phases, such as amphibole or mica, have been reported to date, although traces of apatite may be present. Characterisation of the lithospheric mantle composition and its evolution however, is hampered by patchy and uneven geochemical analyses across the xenolith suite. Nonetheless, a picture emerges of a heterogeneous lithosphere beneath both Ross and Amundsen Provinces. Previously published and new data reported here are consistent with samples ranging from variably cryptically metasomatised residua from variable (10 – 25%) degrees of partial melt extraction to refertilised compositions. Limited isotopic data point to a complex history, providing evidence for both ancient Proterozoic lithospheric mantle and preservation of Ordovician events. The Sr-Nd-Pb composition of the sampled lithospheric mantle overlaps the common low-μ isotopic endmember identified in Cenozoic magmatism from MBL and the wider West Antarctic Rift System.

Supplementary material: Analytical methods, and Literature sources for off-cratonic spinel peridotite whole rock data (MS word file); Data Tables: 1. Mineral major element data; 2. Mineral trace element data; 3. Whole rock major element data; 4. Whole rock trace element data (MS Excel file).

Introduction

Marie Byrd Land forms one of four major crustal blocks comprising the composite West Antarctica (Figure 1a). For much of its evolution Marie Byrd Land was part of the paleo-Pacific Gondwana margin and in this setting experienced a protracted Paleozoic history defined by convergence and subduction (Figure 1b). Currently however, it forms the northern flank of the West Antarctic Rift System (WARS), a continental rift complex that initiated in the late Cretaceous and now extends for over 2500 km along the eastern margin of the Antarctic continent from Cape Adare to the base of the Antarctic Peninsula (Figure 1a; Le Masurier and Thomson, 1990; Storey *et al*. 1999; Jordan *et al.* 2020). As part of the WARS, Marie Byrd Land has been a focus for intraplate volcanism dating back at least 37 Ma (LeMasurier and Thomson, 1990, Kyle and Muncy, 1989, Smellie, *et al.,* 2020; Panter *et al.,* in press).

Much of West Antarctic surface geology is obscured by extensive ice sheets, and over large tracts of country only the peaks of basanite-trachyte–phonolite stratovolcanoes (e.g. Mount Sidley, 4285 m) are exposed through the veneer of ice (e.g. Figure 1). Surface exposure is particularly limited in Marie Byrd Land. However, basanitic scoria cones associated with and peripheral to the major Cenozoic stratovolcanoes are commonly host to diverse suites of xenoliths comprising upper-crustal (granitoids and metamorphic rocks), lower-crustal (mafic and felsic granulites) and mantle (spinel facies peridotites and pyroxenites) xenoliths, and megacrysts, thereby providing key insights into the composition and history of the deeper lithosphere.

Lithospheric mantle xenoliths have been described from several Marie Byrd Land Cenozoic volcanic centres in the Executive Committee Range, Usas Escarpment, and Fosdick Mountains, and from the coastal Mount Murphy (Figure 1), although limited mineralogy and geochemical data have been reported to date (Wysoczanski and Gamble, 1992; Wysoczanski, 1993; Handler *et al*. 2003; Cohen, 2016; Chatzaras *et al*. 2016). This contribution presents a review of the composition and petrogenesis of Marie Byrd Land lithospheric mantle as discerned from the record of mantle xenoliths entrained in Cenozoic magmas, summarising the available literature data and reporting previously unpublished mineral and isotopic data on subsets of the xenoliths.

Geological Setting

Prior to ca. 85 Ma, Marie Byrd Land was contiguous with New Zealand (Zealandia) as part of the Gondwana margin, linking eastern Australia with the Antarctic Penninsula and South America (Jordan, *et al.* 2020; Smellie *et al.* 2020). This margin was characterised by a prolonged period of convergence with magmatic arc(s) represented by Devonian to Late Cretaceous peraluminous, calc-

alkaline series granites now exposed in coastal Marie Byrd Land (Larter *et al*. 2002). The granitoids intrude Neoproterozoic to lower Paleozoic metamorphic basement (Pankhurst *et al.* 1998; Mukasa and Dalziel, 2000).

Marie Byrd Land basement has been divided into two terranes on the basis of differing granite Nd model ages: the Ross Province to the south (T_{DM} ~ 1.5 – 1.3 Ga), and the Amundson Province to the north (T_{DM} ~ 1.3 - 1.0 Ga) (Pankhurst *et al*. 1998) (Figure 1). In central Marie Byrd Land, compositional differences in lower crustal xenoliths from the Executive Committee Range are consistent with the definition of these two crustal terranes and likely constrain their boundary to between mounts Sidley and Hampton (Wysoczanski *et al*. 1995; Figure 1). Paleomagnetic data suggest that these two provinces have shared a common history since mid-Cretaceous times, prior to the separation of Marie Byrd Land and Zealandia (DiVenere *et al*. 1996; Luyendyk *et al*. 1996).

The age of the basement to Marie Byrd Land remains enigmatic however, with the only direct samples of lower crustal rocks proving resistant to dating techniques (Wysoczanski, 1993; Wysoczanski *et al*. 1995). The oldest crustal unit exposed in the Ross Province is the Neoproterozoic to lower Paleozoic Swanson Formation, which has been correlated with metaturbidites in western New Zealand and Northern Victoria Land, (e.g. Figure 1b) (Adams, 1986; Pankhurst *et al*. 1998), and lower Paleozoic gneissic crystalline basement is exposed in the vicinity of Mount Murphy (Figure 1a) (Pankhurst *et al*. 1998, Jordan, *et al.* 2020). The Amundsen Province has been correlated with the Zealandia Median Batholith in New Zealand, with the oldest known crustal rocks Ordovician-Silurian calc-alkaline granitoids (e.g. Pankhurst *et al*, 1998; Smellie *et al*. 2020).

Proterozoic ages associated with the widespread granitoid suites – both whole-rock Nd model ages and U-Pb ages of inherited zircon – have been used to suggest that Proterozoic basement underlies Marie Byrd Land's two provinces (e.g. Pankhurst *et al*. 1998; Mukasa & Dalziel, 2000), apparently supported by Proterozoic Os model ages in mantle peridotite xenoliths from the Executive Committee Range (Handler *et al*. 2003). However, the granite model ages and zircon core ages could equally be explained by contributions from the thick lower Paleozoic turbidite deposits sourced from Proterozoic terranes (Pankhurst *et al*. 1998), and Proterozoic mantle has been reported from Phanerozoic crustal terranes, oceanic plateau and subduction zones elsewhere (e.g. Hassler and Shimizu, 1998; Parkinson *et al*. 1998; McCoy-West *et al*. 2013). Lower crustal xenolith Pb isotope data are more consistent with Phanerozoic ages (Wysoczanski, 1993).

The middle Cretaceous marked a period of extension (e.g. Weaver *et al*. 1992,1994; Luyendyk *et al*. 1996) associated with the break-up of this portion of the Gondwana margin. Evidence for pre-break-

up rifting offshore Marie Byrd Land has been documented from ca. 96 Ma, with Marie Byrd Land-Zealandia break-up estimated ca. 84 - 80 Ma (Wobbe *et al*. 2012; LeMasurier *et al*. 2016; Tulloch *et al.* 2019). Coastal Marie Byrd Land is characterised by basin and range style faulting, attenuated crust and alkaline volcanism (LeMasurier *et al*. 2016; Heinemann *et al*. 1999; LeMasurier, 2008; LeMasurier and Landis, 1996). Crustal thickness is estimated to be 22 – 33 km (Chaput *et al*. 2014) with the lithosphere extending to depths of 80 – 100 km (An *et al*. 2015).

The Cenozoic Marie Byrd Land intraplate volcanic province forms a 1000 x 550 km tectonomagmatic dome centered near Mount Flint (Figure 1a). Active since ca. 36 Ma, the volcanic province is dominantly mafic in nature with felsic volcanism apparent since ca. 19 Ma (Hole and LeMasurier, 1994; Panter, 1997; Winberry and Anandakrishnan, 2004; LeMasurier *et al*. 2016; Panter *et al.* in press). All but two of 18 identified shield-like composite volcanoes are partially buried within the West Antarctic Ice Sheet with mainly the summit regions exposed (e.g. LeMasurier, 2013), and additional volcanic centres are fully buried beneath the West Antarctic Ice Sheet (Van Wyk de Vries *et al*. 2017).

Xenolith locations and sample datasets

Lithospheric mantle xenoliths, typically 2–6 cm in diameter but ranging up to ~20 cm, have been described from Mount Murphy (on the Walgreen Coast), Mount Aldaz (in the Usas Escarpment), and several volcanic centres in the Executive Committee Range and Fosdick Mountains as part of two PhD and MSc theses (Wysoczanski, 1993; Cohen, 2016; Table 1). Moreover, additional geochemical, isotopic and/or textural and imaging data are reported in Handler *et al*. (2003), Chatzaras *et al*. (2016) and Chatzaras and Kruckenberg (this volume). Whilst limited to volcanic centres that protrude the ice sheet, the xenolith sites are sufficiently distributed to sample lithosphere beneath the Ross Province (Fosdick Mountains), the Amundsen Province (Mounts Cumming, Hampton and Aldaz) and in the vicinity of the boundary between the two (Mount Murphy; Mount Hampton) (Figure 1).

Over 100 upper mantle xenoliths have been reported from across Marie Byrd Land, however the data available for the xenoliths is varied and uneven. The xenolith suites described by Cohen (2016) and Chatzaras *et al*. (2016) come dominantly, but not exclusively, from the Fosdick Mountains and provide a wealth of textural and mineral major element data. By contrast, data for the upper mantle xenolith suites reported by Wysoczanski (1993), whose main thesis focus was on lower crustal xenoliths, are largely limited to whole rock major element chemistry. Small subsets of the xenolith suites from the Executive Committee Range, Fosdick Mountains and Usas Escarpment have been analysed for mineral major and trace element data, or whole rock isotopes (Sr, Nd, Pb and Os), much

of which has not been previously reported (the exception being Os isotopic data and limited major elements, in Handler *et al*. 2003). In addition, a spinel lherzolite from Mount Hampton (PK91005) was the focus of a study on cosmogenic helium and neon in older mantle samples (Moreira and Madureira, 2005).

Petrography and Mineral Chemistry

The upper mantle xenolith suite is dominated by Type 1 peridotites (Frey and Prinz, 1978), predominantly spinel lherzolite but also harzburgite and dunite compositions (Wysoczanski, 1993; Cohen 2016). Rarer clinopyroxenite (Mount Hampton, Mount Aldaz, Demas Bluff), and websterite and wehrlite (Fosdick Mountains) xenoliths have also been reported (Wysoczanski, 1993; Cohen, 2016; Figure 2). Clinopyroxenite xenoliths from Mount Hampton contain Cr-diopside chemically identical to those found as mm-scale veins cross-cutting lherzolite samples from the same locality and are interpreted to represent fragments of larger, cm- to dm-scale, veins (Wysoczanski, 1993). Clinopyroxene-rich veins are also observed cross-cutting lherzolite xenoliths from the Usas Escarpment (e.g. MB69B; Figure 3) and a clinopyroxenite xenolith has also been reported from this locality (AD6021-X01; Cohen, 2016).

The sampled lithospheric mantle appears to be anhydrous with a mineral assemblage restricted to olivine + enstatite ± chrome-diopside + chrome-spinel; metasomatic hydrous phases, such as amphibole and mica, have not been reported in any xenoliths studied to date. Garnet is also absent.

The xenoliths have metamorphic textures and are dominantly coarse-grained granular and tabular, with porphyroclastic textures present but less common (e.g. Figure 3; Wysoczanski, 1993; Cohen, 2016). Olivine and orthopyroxene are generally present as larger grains, commonly reaching up to 6 mm or 5mm, respectively, and up to ~ 9 mm in a few xenoliths from Demas Bluff, Fosdick Mountains (e.g. Cohen, 2016). The average olivine and orthopyroxene grain sizes for individual samples vary from 100–2000 μm and 90–1200 μm, respectively (Wysoczanski, 1993; Cohen, 2016). Clinopyroxene is typically finer than olivine and orthopyroxene, except where veining is apparent, and is commonly associated with spinel. Average clinopyroxene grain size varies from ~ 75–860 μm (Wysoczanski, 1993; Cohen, 2016).

Olivine porphyroclasts show strain features (dislocation boundaries and subgrains) and curvilinear boundaries, with kinkbands common in larger olivine grains across the suite (e.g. Figure 3). Larger pyroxene grains can show deformation twinning or exsolution lamellae, including those within veins (e.g. MB69B vein, Figure 3) and in pyroxenites. Smaller, recrystallised neoblasts are generally dislocation-free and commonly characterised by curvilinear boundaries (e.g. 90040E; Figure 3), in

places attaining 120° triple junctions (e.g. PK4A1; Figure 3). Spinel grains are typically interstitial and randomly distributed, although spinel trails have been observed in some xenoliths from the Fosdick Mountains (Cohen, 2016), as well as larger, "holly-leaf" spinel grains. Detailed textural descriptions of the Fosdick Mountains suite can be found in Cohen (2016) including grain-size distributions, with deformation and crystallographic orientation analyses presented in Cohen (2016) and Chatzaras *et al*. (2016).

Mineral major element compositions (Figure 4) are reported for 41 xenoliths in Chatzaras *et al.* (2016). Olivine and pyroxene compositions for an additional seven xenoliths are reported here (Supplementary file), with representative analyses shown in Table 2.

Olivine compositions are Mg-rich with 100.Mg/(Mg+Fe^{2+}) (Mg#) ranging from 88 – 92, within the range of mantle compositions, with the exception of one sample from Demas Bluff (FDM-DB02-X06, Mg# = 83.4; Chatzaras *et al*., 2016). All analysed olivine have low CaO [< 0.2 weight percent (wt%)] and NiO ranges from 0.3 – 0.5 (wt%). Orthopyroxene compositions parallel those of coexisting olivine, with compositions showing a range in Mg# from 89 – 93. Clinopyroxene have Mg# ranging from 89 – 95 (excluding FDM-DB02-X06), and Cr_2O_3 = 0.1 – 1.9 wt%.

All peridotite samples for which both spinel and olivine data are available, aside from a dunite xenolith from Mount Cumming, plot on the olivine-spinel mantle array (Figure 4) consistent with the suite representing residua from varying degrees of partial melting. Spinel Cr# [100.Cr/(Cr+Al)] ranges between ~ 6 – 40. The Mount Cumming dunite contains two populations of spinel (high- and low-Cr) and has olivine–spinel compositions indicative of melt interaction rather than being residual from large degrees of partial melting (Figure 4; Cohen, 2016). Plots of Al_2O_3 and MgO are shown for both clinopyroxene and orthopyroxene for the xenolith suite (Figure 4), with negative trends that are broadly compatible with up to 15–20% depletion of spinel-facies mantle for the bulk of the suite. In detail however, many of the clinopyroxene from the Fosdick Mountains scatter to higher Al_2O_3 contents (Figure 4).

Trace element concentrations, as determined by laser ablation–inductively coupled plasma mass spectrometry or instrumental neutron activation analysis on mineral separates (see Supplementary files) for olivine, orthopyroxene and clinopyroxene for six peridotites are shown in chondrite-normalised (N) rare earth element (REE) diagrams (Figure 5) and primitive-mantle normalised multielement diagrams (Figure 6). Minerals have been analysed from xenoliths from two locations in the coastal ranges of Marie Byrd Land (West Recess Nunatak and Demas Bluff, Fosdick Mountains,

Ross Province), and three from central Marie Byrd Land (Mount Hampton and Mount Cumming, Executive Committee Range, and Mount Aldaz, Usas Escarpment, Amundsen Province). Samples from the Fosdick Mountains and Mount Aldaz are light (L)REE depleted with convex upward REE patterns for the clinopyroxenes ($[Ce/Sm]_N$~0.4) and generally flat heavy (H)REE ($[Sm/Yb]_N$ ~ 1.0). Incompatible trace element plots of clinopyroxene from Demas Bluff and Recess Nunatak are very similar, showing depletions in the highly incompatible trace elements relative to the slightly less incompatible trace elements (Figure 6). Both patterns show distinctive negative Ba- and Ti-anomalies. The LREE-depleted patterns are consistent with variable degrees of partial melt extraction, however despite preserving LREE-depleted patterns the samples show evidence of open system behaviour. The LREE (La + Ce and in some examples Nd), are out of equilibrium between coexisting clinopyroxene and orthopyroxene (Figure 7), suggestive of cryptic metasomatism.

Clinopyroxene from Mounts Cumming and Hampton in the Executive Committee Range have variable REE patterns ranging from LREE depleted, similar to those of the Fosdick Mountains, to LREE enriched (Figure 5). Clinopyroxene from Mount Cumming sample 1998 and Mount Hampton sample 2000/12 show convex upward REE patterns with $(Ce/Sm)_N$ = 0.7 and 0.3 respectively (Supplementary file). Clinopyroxene from Mount Hampton sample 91005 and Mount Cumming sample 2000/2 have a concave upward REE pattern that is commonly interpreted as indicating metasomatic enrichment of LREE (e.g. McDonough & Frey, 1989; Blusztajn & Shimizu, 1994; Baker et al., 1998). Despite the very different REE profiles, the coexisting clinopyroxene and orthopyroxene in the two Mount Hampton xenoliths appear to be in equilibrium (Figure 7). By contrast, La + Ce + Nd are strongly out of equilibrium in the LREE-enriched Mount Cumming xenolith (2000/2; Figure 7). The multielement plots of clinopyroxene from the LREE enriched Mount Hampton and Mount Cumming samples (91005, 2000/2) also show complex patterns, with both showing marked Zr-Hf depletions, and enrichments in Th and U relative to the LREE-depleted samples from these sites (1998, 2000/12; Figure 6). Both Mount Hampton samples show distinctive Ti anomalies, which are less evident in the samples from Mount Cumming.

Whole rock geochemical composition

Whole rock major element data are reported for 59 xenoliths from mounts Cumming (11) and Hampton (27) in the Executive Committee Range, Mount Aldaz (8), and Mount Murphy (13) with a limited range of trace element data reported for a subset of these (Wysoczanski, 1993; see Supplementary file). Whole rock major element compositions are broadly consistent with the samples representing residual compositions following variable degrees of melt extraction (Figure 8). Low P_2O_5 contents in most samples (< 0.05 wt%) are consistent with an absence of secondary apatite

(Supplementary file), however one Mount Hampton peridotite (PKO) has 0.10 wt% P_2O_5, suggesting traces of apatite may be present. A number of the peridotites scatter to high FeO_{Total} contents, most notably the Mount Murphy suite, and to high Na_2O, suggestive of secondary processes. These may be related to host basanite infiltration, which has also affected lower crustal xenoliths (Wysoczanski, 1993), or refertilisation within the lithospheric mantle via interaction with Fe-rich melts.

Strontium, Nd and Pb isotopes have been measured for a suite of xenoliths from central Marie Byrd Land (mounts Hampton, Cumming and Aldaz). These are reported in Table 3 and plotted on standard covariation diagrams in Figure 9. On the Sr versus Nd isotope diagram, data from the Executive Committee Range and Usas Escarpment (uncorrected for age) plot in the depleted mantle field, clustering close to the HIMU ["high-μ", where $\mu=(^{238}U/^{204}Pb)_{t=0}$; Stracke *et al.* 2005] mantle end-member, as do data from Executive Committee Range lava flows. A single sample from the Usas Escarpment (MB69E) has highly depleted characteristics (εNd = +22.9; $^{87}Sr/^{86}Sr$ = 0.70191). In $^{208}Pb/^{204}Pb$ versus $^{206}Pb/^{204}Pb$ space, the bulk of the data cluster around and below the Northern Hemisphere Reference Line (NHRL; Hart, 1984), and overlap with the less radiogenic compositions of Marie Byrd Land mafic volcanic rocks (Figure 9).

Osmium isotopic data for 17 xenoliths from mounts Aldaz, Hampton and Cumming were reported in Handler *et al*. (2003) with Re-Os data for an additional two samples from the Fosdick Mountains reported here (Table 3). The $^{187}Os/^{188}Os$ data for all but one xenolith range from depleted to values close to primitive upper mantle estimates (0.1162 – 0.1288), consistent with a time-integrated history of variable melt depletion (e.g. CaO ranging from 0.4 – 3.4 wt%). A single sample from Mount Aldaz however, has a superchondritic composition (MB69F; $^{187}Os/^{188}Os$ ~ 0.132).

Petrogenesis and regional variability

Geothermobarometry

Chatzaras *et al*. (2016) reported two-pyroxene equilibrium temperatures for 41 xenoliths, predominantly from sites in the Fosdick Mountains (Figure 10). Preferred temperature estimates were taken as the average of three two-pyroxene thermometers (Bertrand and Mercier, 1985; Brey and Köhler, 1990; Taylor, 1998) calculated at 1.5 GPa, which were all in close agreement. In the absence of a reliable geobarometer for spinel peridotite compositions, pressures were estimated using a theoretical geotherm constructed such that all xenoliths were at pressures consistent with being below the crust and within the spinel stability field, and subparallel to the present day Ross Embayment geotherm of ten Brink *et al*. (1997) (Chatzaras *et al*., 2016).

Equilibration temperatures based on the coexisting clinopyroxene and orthopyroxene (Wells, 1977; Brey and Köhler, 1990; Putirka, 2008; Liang *et al*., 2013) for an additional eight xenoliths are reported here in Table 4. Temperatures calculated using the Putirka (2008) thermometer are consistently higher than those calculated using the Wells (1977) or Brey and Köhler (1990) thermometers, although the Mount Hampton and Demas Bluff samples agree within uncertainties across the thermometers. The xenolith from West Recess Nunatak shows the highest discrepancy between temperature estimates, suggesting that the analysed pyroxenes in this sample are not fully in equilibrium. Rare earth element data were obtained for coexisting clinopyroxene and orthopyroxene for five of the xenoliths, allowing the application of the Liang *et al*. (2013) REE geothermometer. For all five samples here, the middle (M) and HREE appear to be in equilibrium for the coexisting pyroxene pairs (Figure 7) and calculated temperatures are in good agreement with the Brey and Köhler (1990) thermometer (Table 4). Notably, the West Recess Nunatak xenolith that produced the inconsistent temperature estimates amongst the major element thermometers also produced very large uncertainties on the REE in pyroxene thermometer estimate (965 ± 105°C).

The temperature estimates are also shown on Figure 10, using the Brey and Köhler (1990) temperatures and hypothetical geotherm of Chatzaras *et al*. (2016) for consistency between the two datasets. Excluding the West Recess Nunatak sample, calculated temperatures are broadly in the range 900 – 1100°C, within the range of temperatures determined for the larger Fosdick Mountain xenolith suite (Chatzaras *et al*. 2016).

There appear to be no obvious differences in temperature between porphyroclastic and protogranular textural varieties, nor by locality. The Demas Bluff xenolith suite, with the largest number of xenoliths analysed, shows the widest range in temperatures and is the only site to include samples with equilibration temperatures significantly higher than 1100°C. Overall however, the different locations have broadly similar temperature ranges, which are largely restricted to temperatures between 800 – 1050°C. This range is consistent with the exsolved nature of pyroxenes in many of the samples and with a generally "cool" nature of stabilised subcontinental mantle lithosphere (e.g. McKenzie *et al*. 2007; Lee, *et al*. 2010).

Melt depletion and refertilisation

Whole rock major element compositions are broadly consistent with being residues from variable degrees of partial melting, however higher FeO_{Total} and Na_2O in some samples suggest secondary processes have also affected these samples (Figure 8). This is particularly evident for the xenolith suite from Mount Murphy, which typically has FeO_{Total} > 10 wt% as well as tending to lower Al_2O_3

relative to MgO than predicted for partial melt extraction from a primitive mantle-like source (Figure 8). However, major element trends very similar to those produced by melt extraction can also be produced by refertilisation of strongly depleted peridotite (e.g. Van der Wal and Bodinier 1996; Bedini *et al*. 1997; Martin *et al*. 2014). Distinguishing the extent to which partial melt extraction or refertilisation of depleted peridotite have affected the sampled Marie Byrd Land upper mantle is hampered by incomplete and patchy datasets for the xenoliths.

Whole rock FeO_{Total} and/or Na_2O data suggest refertilisation may have affected at least some of the sampled lithospheric mantle, particularly that sampled at Mount Murphy. Trace element data are available for two Mount Murphy xenoliths, which have relatively low FeO_{Total} contents (8.9 - 9 wt% compared to others that are up to ~14 wt%) for this locality (Supplementary file). These have LREE enriched patterns ($[La/Yb]_N$ = 2.0-3.0), consistent with interaction with moderately LREE-enriched melts.

Limited whole rock trace element data are available for a subset of the xenoliths (Supplementary file). Of these, three lherzolites from Mount Aldaz (2) and Mount Cumming (1) have whole rock LREE-depleted patterns with $[La/Yb]_N$ = 0.15 – 0.69 and Yb = 0.05 – 0.09 parts per million (ppm), consistent with residues from partial melting in spinel facies, however most analysed samples have elevated L-MREE consistent with enrichment processes (e.g. $[La/Yb]_N$ ~ 1 – 5.9). The range of HREE are consistent with most of the lherzolite samples analysed having experienced <10% partial melt extraction in spinel facies (e.g. Yb = 0.26 – 0.42 ppm), with three samples from Mount Hampton and one from Mount Cumming preserving low Lu and Yb concentrations more consistent with up to ca. 20% partial melt extraction (e.g. Yb = 0.02 – 0.09 ppm).

Pyroxene major element chemistry is also broadly consistent with the bulk of the suite being residual from < 20% partial melt extraction, with a few harzburgites and lherzolites from the Fosdick Mountains ranging to 25%, based on theoretical melting trends from a primitive upper mantle source (Upton *et al*. 2011; Figure 4). In detail however, co-existing orthopyroxene and clinopyroxene suggest differing degrees of melt extraction for many of the xenolith suite. For example, clinopyroxenes from Fosdick Mountains lherzolite samples reported in Chatzaras *et al*. (2016) extend to higher Al_2O_3 and lower MgO contents than the primitive upper mantle starting composition, and the composition of Mount Hampton and Mount Cumming clinopyroxenes reported here suggest higher degrees of melting than their respective orthopyroxenes. Discrepancy between melt extraction estimates derived from coexisting pyroxenes in spinel lherzolite xenoliths elsewhere has been used to suggest a more complex history involving refertilisation of strongly depleted peridotite

(e.g. Upton *et al*. 2011). However, the compositions of pyroxenes from the two xenoliths from the Fosdick Mountains do provide consistent melt extraction estimates (Figure 4).

Modeling of partial melting based on REE in clinopyroxene for six of the seven xenoliths that data are available for are broadly consistent with 2 – 15 % fractional melting or 2 – 22% batch melting of a primitive upper mantle source in spinel facies (Figure 11). One Mount Cumming xenolith (1998) has a distinctly HREE depleted, convex upward REE pattern suggestive of partial melting with garnet present (e.g. Bonadiman *et al*. 2005), with subsequent reequilibration within spinel facies in the lithosphere (e.g. $[Gd/Yb]_N$ ~2.8 versus ~0.6 at similar Yb contents; Figure 11a, b). The Fosdick Mountains xenoliths and one Mount Hampton sample (2000/12) also have a less pronounced convex up REE pattern that suggests there may have been some influence of garnet during partial melting (e.g. Fosdick Mountains and Mount Hampton 2000/12 $[Gd/Yb]_N$ = 1.3 – 1.7) perhaps in the first stages of polybaric melt extraction. Coupled Cr_2O_3 and CaO contents of clinopyroxene in these samples and across the wider xenolith suite, however, are generally consistent with spinel lherzolite rather than garnet peridotite precursor (e.g. Bonadiman *et al*. 2005).

Overall, the lithospheric mantle, as sampled, is heterogeneous both within and across localities and terranes, and likely preserves a mixture of variably cryptically metasomatised (e.g. LREE enriched) mantle residues, and more depleted samples that underwent subsequent refertilisation to produce fertile lherzolite compositions.

A large number of the xenoliths from within the Ross Province (Fosdick Mountains) have pyroxene mineral compositions suggestive of refertilisation of a harzburgitic source: high Al_2O_3 in many clinopyroxenes, and orthopyroxene and clinopyroxene major element compositions consistent with different estimates for degree of partial melt extraction. However, some samples preserve clinopyroxene and orthopyroxene chemistry consistent with larger (20 – 25%) degrees of partial melt extraction.

Within the Amundsen Province sites, samples from Executive Committee Range typically show smaller discrepancies between major element pyroxene partial melting estimates, and variable REE patterns broadly consistent with the major elements (e.g. 91005 higher degrees of melt extraction than 2000/12; Figure 4b,c; Figure 11c,d). One sample from Mount Cumming retains a REE pattern in clinopyroxene suggestive of the influence of garnet in its melting history. By contrast, Mount Aldaz xenolith whole rock and clinopyroxene REE data are consistent with low degrees of partial melting in the spinel facies (e.g. Figure 4e,f).

Only whole rock data are available for xenoliths from Mount Murphy, in the boundary region between the two provinces, and of all the xenoliths suites, the chemistry for these is the least consistent with a simple melt extraction history.

Metasomatism

Whilst there is an absence of secondary minerals reported for the xenolith suite, major and trace element data record interaction of the peridotites with metasomatic fluids and/or melts (Figures 4 – 8). Characterising the nature and extent of these interactions is hampered by the limited trace element and isotopic data available. However, some constraints can be determined from the trace element profiles of clinopyroxene from the six samples from the Executive Committee Range and Fosdick Mountains (Figure 6), which point to varied metasomatic agents influencing the lithospheric mantle.

Clinopyroxene from three spinel lherzolite samples show variable and elevated L-MREE patterns and enrichments in Th and U (1998 and 2000/2 from Mount Cumming, and 91005 from Mount Hampton; Figure 6). Relative depletions in Zr, Hf and Ti, and Rb and Ba, will at least in part reflect that, unlike the REE, these elements partition more strongly into co-existing spinel than clinopyroxene (e.g. Grégoire *et al*. 2000; Bonadiman *et al*. 2005).

Relatively high Pb/Ce ratios for the incompatible trace element enriched Mount Cumming sample 2000/2 [$(Pb/Ce)_N$ ~ 3-10] compared with the incompatible trace element depleted samples [Mount Hampton 2000/12 and Demas Bluff; $(Pb/Ce)_N$ ~ 0.5 – 1], coupled with strong enrichments in Th, U and depleted Nb and Ta, are consistent with interaction with a melt or fluid bearing a subduction signature. By contrast, the incompatible trace element enrichment pattern in sample 91005 from Mount Hampton shows stronger enrichments in L-MREE and Nb, but lesser enrichments in Th and U (Ta and Pb were not measured), suggesting interaction with melts of a differing origin. This sample also has high Eu/Ti (Figure 6), which is a signature attributed to interaction with carbonatitic melts (e.g. Yaxley *et al*. 1991; Scott *et al*. 2014; Martin *et al.* 2015). Notably, the Mount Cumming xenoliths with high Th, U and low Nb and Ta do not have elevated Eu/Ti.

Age and source characteristics

Re-Os data of xenoliths from the Amundsen Province sites (mounts Hampton, Cumming and Aldaz) provide mantle depletion age constraints consistent with Proterozoic stabilisation of the lithosphere (1.3 – 1.1 Ga), and coincident with Nd model ages of the granitoids of the Amundsen Province (1.3 – 1.0 Ga, Pankhurst *et al*. 1998; Handler *et al*. 2003).

Two additional Re-Os data for samples from Fosdick Mountains, Ross Province, also return Proterozoic model ages, with one sample overlapping those from the Amundsen Province samples and the second significantly less radiogenic sample, yielding an older Re depletion age of ca. 1.7 Ga (Table 3). This is even older than the Nd model ages of granitoids of the Ross Province (1.5 – 1.3 Ga), suggesting that the crust is younger than the mantle, which contains older Proterozoic foundations or perhaps remnants of older mantle caught up during continent formation. If the Nd model ages (and U-Pb ages of inherited zircon) in the granitoids reflect a recycled sediment source rather than crust formation ages, the discrepancy between mantle and crustal ages may be quite significant. Isolated, ancient mantle domains decoupled from younger overlying crust have been reported from other terranes along the eastern Gondwana margin, most notably from Zealandia (e.g. McCoy-West *et al*. 2013; Liu *et al*. 2015).

But not all of the xenolith isotopic data point to Proterozoic ages. In detail, the Mount Aldaz samples have isotopic systematics that are more consistent with an influence from the prolonged history of Paleozoic subduction known to have affected Marie Byrd Land. Three of the four xenoliths from Mount Aldaz have Os concentrations [3.2-3.7 parts per billion (ppb)] and isotopic compositions ($^{187}Os/^{188}Os$ ~ 0.125 – 0.128; Handler *et al.* 2003) that span estimates of modern primitive and depleted upper mantle compositions (e.g. Meisel *et al*. 1996; Brandon *et al*. 2000; Day *et al*. 2017), producing relatively young Re-depletion model ages (570 – 130 Ma). One of these samples, MB69E, also preserves extremely depleted $^{87}Sr/^{86}Sr$ and $^{143}Nd/^{144}Nd$ compositions (Figure 9a). This sample has a Nd depleted mantle model age of ca. 488 Ma, broadly in agreement with its Re depletion age of ca. 420 Ma. Both ages are consistent with material added to the lithospheric mantle during the Ordovician, a time of convergence and subduction magmatism along the Gondwana margin (e.g. Pankhurst *et al*. 1998). The fourth xenolith from Mount Aldaz (MB69F) has a radiogenic Os isotopic composition ($^{187}Os/^{188}Os$ ~ 0.132), coupled with lower Os content (~ 1.5 ppb; Handler *et al*. 2003). These characteristics are consistent with radiogenic Os addition such as has been described for suprasubduction zone modified peridotites (e.g. Brandon *et al*. 1996) and chromites (Suzuki *et al*. 2011) elsewhere. In addition, these ages closely overlap the timing of suggested pyroxenite emplacement and metasomatism in the adjacent Victoria Land lithospheric mantle, as evidenced by ages for a clinopyroxenite xenolith from Foster Crater (McGibbon, 1991) and eclogite and carbonatite emplacement in Victoria Land (Martin *et al*. 2015).

Aside from MB69E with its strongly depleted Sr and Nd isotopic composition, the sampled central Marie Byrd Land lithospheric mantle has a Sr-Nd-Pb isotopic composition that broadly overlaps an endmember identified in several studies of Cenozoic mafic volcanism across Marie Byrd Land and

the Ross Sea region (Figure 9). This isotopic endmember, variously described as low-μ or FOZO ("FOcal ZOne"; Stracke *et al.* 2005), appears to be a common component in much of the Cenozoic volcanism across the WARS (e.g. Hart *et al*. 1997; Panter *et al*. 2000; Aviado *et al*. 2015). Similar $^{87}Sr/^{86}Sr$ and $^{143}Nd/^{144}Nd$ compositions have also been reported for pyroxenite xenoliths from Marie Byrd Land (Wysoczanski *et al*. 1995) and upper mantle peridotite from Victoria Land (Martin *et al*. 2013), consistent with a widespread nature of this common signature in the lithospheric mantle across the wider region (e.g. Panter *et al*. 2000). The origin of this low-μ signature has been variously attributed to metasomatic enrichment of lithospheric mantle by both subduction and intraplate related magmatism (e.g. Day *et al*. 2019; Panter *et al*. 2000; LeMasurier *et al*. 2016). Although very limited, trace element data for clinopyroxene from Marie Byrd Land mantle xenoliths are consistent with either or both of these mechanisms influencing the sampled lithospheric mantle. Furthermore, as noted, the age and Os isotopic composition of some Mount Aldaz peridotites are consistent with lithospheric mantle influenced by subduction zone magmatism. However, there is no evidence for hydrous phases in the Marie Byrd Land lithospheric mantle sampled to date, as had been proposed from studies of volcanic rocks (e.g. Panter *et al*. 2000; LeMasurier *et al*. 2016) and the source of this hydrous component in the source of the Cenozoic magmatism in Marie Byrd Land remains elusive. This is in apparent contrast with lithospheric mantle xenolith suites from adjacent terranes, for example southern Victoria Land, where hydrous phases such as phlogopite and amphibole have been reported in lithospheric mantle xenoliths (e.g. Gamble *et al*. 1988; Martin *et al*. 2014; Day *et al*. 2019) although not all xenolith locations in southern Victoria Land contain hydrous mineral bearing xenoliths; the xenolith suite from Mount Morning is anhydrous (Martin *et al.* 2015).

Cenozoic basaltic magmatism from Marie Byrd Land points to a mixing between this low-μ source and a HIMU endmember (e.g. Panter *et al*. 2000) that has been observed in magmatism more broadly in the southwest Pacific (e.g. McCoy-West *et al*. 2010; Gamble *et al.* 2018; Smellie *et al*. 2020). There is no evidence for a HIMU signature preserved in the sampled lithospheric mantle, nor in lower crustal or pyroxenite samples (Wysoczanski *et al*. 1995) analysed to date. This would be consistent with a compositionally layered mantle beneath Marie Byrd Land whereby a HIMU (fossil plume?) component underplates the lithospheric mantle, such as has been postulated in several studies (e.g. Weaver *et al.* 1994; Panter *et al*. 2000; Kipf *et al.* 2014). Direct samples of this mantle material have yet to be documented however.

Summary and Conclusions

Cenozoic mafic magmatism has carried a large suite of lithospheric mantle xenoliths to the surface, from localities within both major terranes, the Ross and Amundsen provinces, that comprise Marie

Byrd Land. The xenoliths are predominantly lherzolitic in composition, but include lesser amounts of harzburgite and rare dunite and pyroxenites. All are spinel-bearing; garnet is absent. No hydrous phases have been documented, although it is likely traces of apatite are present in at least a few samples. The sampled lithosphere is typically coarse granular to porphyroclastic, with pyroxenite veining present. Equilibration temperatures fall largely within 800 – 1050°C, with no apparent temperature variation with textural variety or by locality.

Characterisation of the lithospheric mantle and unravelling its age and evolution is hampered by patchy analytical datasets across the suite, and in particular, a lack of fully characterised samples from any single locality. Nonetheless, what emerges is a heterogeneous lithospheric mantle, likely preserving residues from various episodes and degrees of melt extraction together with refertilised material, and the influence of a variety of secondary cryptic metasomatic processes. Isotopically, the Marie Byrd Land lithospheric mantle is consistent with a low-μ (FOZO) component recognised in Cenozoic magmatism across the region. Limited Re-Os data suggest preservation of ancient, Proterozoic lithospheric mantle beneath both Ross and Amundsen provinces that may pre-date the overlying crust. However, isotopic data also indicate the influence of younger events, most notably Ordovician Os and Nd model ages for a lherzolite xenolith from the Usas Escarpment, Ross Province, that are consistent with a lithospheric mantle influenced by the protracted history of Paleozoic convergence and subduction.

Acknowledgements

Xenoliths were collected during Antarctic expeditions supported by NSF-DPP, Antarctica New Zealand and VUWAE in 1982, 1983, 1984, 1988, 1989, 1990 and 1992, with the majority collected as an objective of the joint NZ – US – UK sponsored WAVE (West Antarctica Volcano Exploration) project that formed the basis of the Wysoczanski (1993) and Handler *et al*. (2003) studies. During the WAVE project field support from Bill McIntosh, Philip Kyle, Kurt Panter, Nelia Dunbar and John Smellie gave valuable assistance. Additional mineral data are reported here for samples donated by Chris Adams (Demas Bluff) and Dave Kimbrough (Recess Nunatak). Strontium, Nd and Pb isotopic data reported here were analysed at DTM, Carnegie Institution of Washington; MRH and RJW thank Rick Carlson, Mary Horan and Tim Mock for their support and assistance. This contribution has benefited from the very thoughtful and constructive comments of Alan Cooper, Adam Martin, and Kurt Panter, and we further thank Adam Martin for his editorial handling.

References

Adams, C.J., 1986. Geochronological studies of the Swanson Formation of Marie Byrd Land, West Antarctica, and correlation with northern Victoria Land, East Antarctica, and South Island, New Zealand. *New Zealand Journal of Geology and Geophysics* 29: 345-358.

An, M., Wiens, D., Zhao, Y., Feng, M.-F., Nyblade, A., Kanao, M., Li, Y., Maggi, A., & Lévêque, J.-J., 2015. S-velocity model and inferred Moho topography beneath the Antarctic Plate from rayleigh waves. *Journal of Geophysical Research: Solid Earth* 120: 359-383. 10.1002/2014JB011332.

Arai, S., 1994. Characterization of spinel peridotites by olivine-spinel compositional relationships: Review and interpretation. *Chemical Geology* 113: 191-204.

Anders, E., & Grevasse, N., 1989. Abundances of the elements: meteoric and solar. *Geochimica et Cosmochimica Acta* 53: 197-214.

Aviado, K. B., Rilling-Hall, S., Bryce, J. G., & Mukasa, S. B., 2015. Submarine and subaerial lavas in the West Antarctic Rift System: Temporal record of shifting magma source components from the lithosphere and asthenosphere. *Geochemistry, Geophysics, Geosystems* 16, 4344–4361, doi:10.1002/2015GC006076.

Baker, J.A., Chazot, G., Menzies, M., & Thirlwall, M., 1998. Metasomatism of the shallow mantle beneath Yemen by the Afar plume–Implications for mantle plumes, flood volcanism and intraplate volcanism. *Geology*, 26: 431–434.

Bedini, R.M., Bodinier, J.-L., Dautria, J.-M., & Morten, L., 1997. Evolution of LILE-enriched small melt fractions in the lithospheric mantle: a case study from the East African Rift. *Earth and Planetary Science Letters* 153: 67-83.

Berg, J.H., Moscati, R.J., & Herz, D.L., 1989. A petrologic geotherm from a continental rift in Antarctica. *Earth and Planetary Science Letters* 93: 98-108.

Bertrand, P., & Mercier, J.-C.C., 1985. The mutual solubility of coexisting ortho- and clinopyroxene: Toward an absolute geothermometer for the natural system? *Earth and Planetary Science Letters* 76: 109-122.

Blusztajn, J., & Shimizu, N., 1994. The trace-element variations in clinopyroxenes from spinel peridotite xenoliths from southwest Poland. *Chemical Geology* 111: 227-243.

Bonadiman, C., Beccaluva, L., Coltorti, M., & Siena, F., 2005. Kimberlite-like metasomatism and 'garnet signature' in spinel-peridotite xenoliths from Sal, Cape Verde archipelago: relics of a

subcontinental mantle domain with the Atlantic Ocean lithosphere? *Journal of Petrology* 46: 2465-2493.

Bradshaw, J.D., Andrews, P.B., & Field, B.D., 1983. Swanson Formation and related rocks of Marie Byrd Land and a comparison with Robertson Bay Groups and Bowers Supergroup, northern Victoria Land, Antarctica. *In:* Oliver, R.L., James, P.R., Jago, J.B. (Eds.), Antarctic Earth Science. Australian Acad. of Sci., Canberra, pp. 274– 279.

Brandon A.D., Creaser, R.A., Shirey, S.B., & Carlson, R.W., 1996. Osmium recycling in subduction zones. *Science* 272: 861-863. doi: 10.1126/science.272.5263.861

Brandon A.D., Snow, J. E., Walker, R.J., Morgan, J.W., & Mock, T.D., 2000. ^{190}Pt–^{186}Os and ^{187}Re–^{187}Os systematics of abyssal peridotites. *Earth and Planetary Science Letters* 177: 319-335.

Brey, G.P., & Köhler, T., 1990. Geothermometry in four-phase lherzolites: II New thermobarometers and practical assessment of existing thermobarometry. *Journal of Petrology* 31:1352-1378.

Chaput, J., Aster, R.C., Huerta, A., Sun, X., Lloyd, A., Wiens, D., Nyblade A., Anandakrishnan, S., Winberry, J.P., & Wilson T., 2014. The crustal thickness of West Antarctica. *Journal of Geophysical Research: Solid Earth* 119:378-395.

Chatzaras, V., Krukenberg, S.C., Cohen, S.M., Medaris Jr, L.G., Withers, A.C., & Bagley, B., 2016. Axial-type olivine crystallographic preffered orientations: The effect of strain geometry on mantle texture. *Journal of Geophysical Research: Solid Earth* 121: 4895-4922.

Cohen, S.M., 2016. An assessment of heterogeneity within the lithospheric mantle, Marie Byrd Land, West Antarctica. MSc. Thesis, Boston College. Pp309.

Day, J.M.D., Harvey, R.P., & Hilton D.R., 2019. Melt-modified lithosphere beneath Ross Island and its role in the tectono-magmatic evolution of the West Antarctic Rift System. *Chemical Geology* 518: 45-54.

Day, J.M.D., Walker, R.J., & Warren, J.M., 2017. ^{186}Os–^{187}Os and highly siderophile element abundance systematics of the mantle revealed by abyssal peridotites and Os-rich alloys. *Geochimica et Cosmochimica Acta* 200: 232-254

DiVenere, V., Kent, D.V., & Dalziel, I.W.D., 1996. Summary of palaeomagnetic results from West Antarctica: implications for the tectonic evolution of the Pacific margin of Gondwana during the Mesozoic. *Geological Society of London Special Publication* 108, 31–43.

Elliot, D.H., 2013. The geological and tectonic evolution of the Transantarctic Mountains: A review. *Geological Society, London, Special Publication* 381, 7-35.

Frey, F.A., & Prinz, M., 1978. Ultramafic inclusions from San Carlos, Arizona: petrologic and geochemical data bearing on their petrogenesis. *Earth and Planetary Science Letters* 38, 129 – 176.

Gamble, J.A., McGibbon, F., Kyle, P.R., Menzies, M.A., & Kirsch, I., 1988. Metasomatised xenoliths from Foster Crater, Antarctica: Implications for lithospheric structure and processes beneath the Transantarctic Mountain front. *Journal of Petrology* Special Lithosphere Issue, p-109-138.

Gamble, J.A., Adams, C.J., Morris, M.A., Wysoczanski, R.J., Handler, M.R., & Timm, C., 2018. The geochemistry and petrogenesis of Carnley Volcano, Auckland Islands, SW Pacific. *New Zealand Journal of Geology and Geophysics*, 61: 480-497.

Grégoire, M., Moine, B.N., O'Reilly, S.Y., Cottin, J.Y., & Giret, A., 2000. Trace element residence and partitioning in mantle xenoliths metasomatized by highly alkaline, silicate- and carbonate-rich melts (Kerguelen Islands, Indian Ocean). *Journal of Petrology* 41: 477-509.

Handler, M. R., Wysoczanski, R. J., & Gamble, J. A., 2003. Proterozoic lithosphere in Marie Byrd Land, West Antarctica: Re–Os systematics of spinel peridotite xenoliths. *Chemical Geology* 196, 131–145.

Hart, S.R., 1984. A large-scale isotope anomaly in the Southern Hemisphere mantle. *Nature* 309: 753-757.

Hart, S.R., Blusztajn, J., LeMasurier, W.E., & Rex, D.C., 1997. Hobbs coast Cenozoic volcanism: Implications for the West Antarctic rift system. *Chemical Geology* 139: 223-248.

Hassler, D.R., & Shimizu, N., 1998. Osmium Isotopic Evidence for Ancient Subcontinental Lithospheric Mantle Beneath the Kerguelen Islands, Southern Indian Ocean. *Science* 280: 418-421.

Heinemann, J., Stock, J., Clayton, R., Hafner, K., Cande, S., & Raymond, C., 1999. Constraints on the proposed Marie Byrd Land – Bellingshausen plate boundary from seismic reflection data. *Journal of Geophyscial Research* 104: 25,321-25,330.

Hole, M.J., & LaMasurier, W., 1994. Tectonic controls on the geochemical composition of Cenozoic, mafic alkaline volcanic rocks from West Antarctica. *Contributions to Mineralogy and Petrology,* 11: 187-202.

Johnston, A.D., & Schwab, B.E., 2004. Constraints on clinopyroxene/melt partitioning of REE, Rb, Sr, Ti, Cr, Zr and Nb during mantle melting: First insights from direct peridotite melting experiments at 1.0 Gpa. *Geochimica et Cosmochimica Acta* 68: 4949-4962.

Jordan, T.A., Riley, T.R., & Siddoway, C.S., 2020. The geological history and evolution of West Antarctica. *Nature Reviews Earth & Environment* 1: 117-133.

Kelemen, P.B., Shimizu, N., & Dunn, T., 1993. Relative depletion of niobium in some arc magmas and the continental crust: Partitioning of K, Nb, La and Ce during melt/rock reaction in the upper mantle. *Earth and Planetary Science Letters* 120: 111-134.

Kipf, A., Hauff, F., Werner, R., Gohl, K., van den Bogaard, P., Hoernle, K., Maicher D., & Klügel, A., 2014. Seamounts off the West Antarctic margin: A case for non-hotspot driven intraplate volcanism. *Gondwana Research* 25: 1660-1679.

Kyle, P.R., & Muncy, H.L., 1989. Geology and geochronology of McMurdo Volcanic Group rocks in the vicinity of Lake Morning, McMurdo Sound, Antarctica. *Antarctic Science* 1: 345-350.

Larter, R.D., Cunningham, A.P., Barker, P.F., Gohl, K., & Nitsche, F.O., 2002. Tectonic evolution of the Paciic margin of Antarctica. I. Late Cretaceous tectonic reconstructions. *Journal of Geophysical Research* 107 (B12): 2345.

Lee, C.-T., Luffi, P., & Chin, E.J., 2010. Building and destroying continental mantle. *Annual Review of Eearth and Planetary Sciences* 39: 59-90.

LeMasurier, W.E., 2008. Neogene extension and basin deepening in the West Antarctic rift inferred from comparisons with the East African rift and other analogs. *Geology* 36: 247-250.

LeMasurier, W., 2013. Shield volcanoes of Marie Byrd Land, West Antarctic rift: oceanic island similarities, continental signature, and tectonic controls. *Bulletin of Volcanology* 75: 726.

LeMasurier, W. E., & Landis, C. A., 1996. Mantle-plume activity recorded by low-relief erosion surfaces in West Antarctica and New Zealand. *Geological Society of America Bulletin* 108: 1450–1466.

LeMasurier, W. E., & Thomson, J. W., 1990. In: *Volcanoes of the Antarctic Plate and Southern Oceans.* American Geophysical Union.

LeMasurier, W.E., Choi, S.H., Hart, S.R., Mukasa, S., & Rogers, N., 2016. Reconciling the shadow of a subduction signature with rift geochemistry and tectonic environment in Eastern Marie Byrd Land, Antarctica. *Lithos* 260: 134–153.

Liang, Y., Sun, C., & Yao, L., 2013. A REE-in-two-pyroxene thermometer for mafic and ultramafic rocks. *Geochimica et Cosmochimica Acta* 102: 246-260.

Liu, J., Scott, J.M., Martin, C.E., & Pearson, D.G., 2015. The longevity of Archean mantle residues in the convecting upper mantle and their role in young continent formation. *Earth and Planetary Science Letters* 424: 109-118.

Luyendyk, B., Cisowski, S., Smith, C., Richard, S., & Kimbrough, D., 1996. Paleomagnetic study of the northern Ford Ranges, western Marie Byrd Land, West Antarctica: motion between West and East Antarctica. *Tectonics* 15: 122–141.

Martin, A.P., Cooper, A.F., & Price, R.C., 2013. Petrogenesis of Cenozoic, alkalic volcanic lineages at Mount Morning, West Antarctica and their entrained lithospheric mantle xenoliths: Lithospheric versus asthenospheric mantle sources. *Geochimica et Cosmochimica Acta* 122: 127–152.

Martin, A.P., Cooper, A.F., & Price, R.C., 2014. Increased mantle heat flow with on-going rifting of the West Antarctic rift system inferred from characterisation of plagioclase peridotite in the shallow Antarctic mantle. *Lithos* 190–191: 173–190.

Martin, A.P., Price, R.C., Cooper, A.F., & McCammon, C.A., 2015. Petrogenesis of the rifted southern Victoria Land lithospheric mantle, Antarctica, inferred from petrography, geochemistry, thermobarometry and oxybarometry of peridotite and pyroxenite xenoliths from the Mount Morning eruptive centre. *Journal of Petrology* 56: 193-226.

McCoy-West, A.J., Baker, J.A., Faure, K., & Wysoczanski, R.J., 2010. Petrogenesis and origins of mid-Cretaceous continental intraplate volcanism in Marlborough, New Zealand: Implications for the long-lived HIMU magmatic mega-province of SW Pacific. *Journal of Petrology* 51: 2003-2045.

McCoy-West, A.J., Bennet, V.C., Puchtel, I.S., & Walker, R.J., 2013. Extreme persistence of cratonic lithosphere in the southwest Pacific: Paleoproterozoic Os isotopic signatures in Zealandia. *Geology* 41: 231-234.

McDonough, W.F., & Frey, F.A., 1989. Rare Earth Elements in upper mantle rocks. *Reviews in Mineralogy* 21: 99-145.

McDonough, W.F., & Sun, S.-S., 1995. The composition of the Earth. *Chemical Geology* 120: 223-253.

McKenzie, D., Jackson, J., & Priestley, K., 2007. Thermal structure of oceanic and continental lithosphere. *Earth and Planetary Science Letters* 233: 337-349.

Meisel, T., Walker, R. J., & Morgan, J. W., 1996. The osmium isotopic composition of the Earth's primitive upper mantle. *Nature* 383: 517-520.

Moreira, M. & Madureira, P., 2005. Cosmogenic helium and neon in 11 Myr old ultramafic xenoliths: Consequences for mantle signatures in old samples. *Geochemistry, Geophysics, Geosystems* doi.org/10.1029/2005GC000939.

Mukasa, S. B., & Dalziel, I. W. D., 2000. Marie Byrd Land, West Antarctica: evolution of Gondwana's Pacific margin constrained by zircon U-Pb geochronology and feldspar common-Pb isotopic compositions. *Geological Society of America Bulletin* 112: 611–627.

Pankhurst, R. J., Weaver, S. D., Bradshaw, J. D., Storey, B. C., & Ireland, T. R., 1998. Geochronology and geochemistry of pre-Jurassic superterranes in Marie Byrd Land, Antarctica. *Journal of Geophysical Research* 103: 2529–2547.

Panter, K.S., 1997. Petrogenesis of a phonolite-trachyte succession at Mount Sidley, Marie Byrd Land, Antarctica. *Journal of Petrology* 38: 1225-1253.

Panter, K.S., Wilch, T.I., Smellie, J.L., Kyle, P.R., McIntosh, W.C., in press. Marie Byrd Land & Ellsworth Land II Petrology. In. J.L. Smellie, K.S. Panter, A. Geyer (Eds), Volcanism in Antarctica : 200 Million Years of Subduction, Rifting and Continental Break-Up. *Geological Society of London Memoir 53.*

Panter, K.S., Hart, S.R., Kyle, P.R., Blusztajn, J., & Wilch, T., 2000. Geochemisty of late Cenozoic basalts from the Crary Mountains: characterization of mantle sources in Marie Byrd Land, Antarctica. *Chemical Geology* 165: 215–241.

Parkinson, I.J., Hawkesworth, C.J., & Cohen, A.S., 1998. Ancient mantle in a modern arc: Osmium isotopes in Izu-Bonin-Mariana forearc peridotites. *Science* 281: 2011-2013.

Putirka, K. D., 2008. Thermometers and barometers for volcanic systems. In. Putirka, K. D., & Tepley, F. J. III, (eds) Minerals, Inclusions and Volcanic Processes. *Mineralogical Society of America and Geochemical Society, Reviews in Mineralogy and Geochemistry* 69: 61-120.

Richard, S.M., Smith, C.H., Kimbrough, D.L., Fitzgerald, P.G., Luyendyk, B.P., & McWilliams, M.O.,

1994. Cooling history of the northern Ford Ranges, Marie Byrd Land, West Antarctica. *Tectonics* 13, 837– 857.

Scott, J.M., Hodgkinson, A., Palin, J.M., Waight, T.E., Van der Meer, Q.H.A., & Cooper, A.F., 2014. Ancient melt depletion overprinted by young carbonatitic metasomatism in the New Zealand lithospheric mantle. *Contributions to Mineralogy and Petrology* 167: 963.

Siddoway, C.S., Richard, S., Fanning, C.M., & Luyendyk, B.P., 2004. Origin and emplacement mechanisms for a middle Cretaceous gneiss dome, Fosdick Mountains, West Antarctica. In: Whitney, D.L., Teyssier, C.T. & Siddoway, C. (eds) Gneiss Domes in Orogeny. *Geological Society of America, Special Papers* 380: 267-294.

Siddoway, C.S., Sass, L.C.III, & Esser, R.P., 2005. Kinematic history of western Marie Byrd Land, West Antarctica: direct evidence from Cretaceous mafic dykes. In. Vaughan, A.P.M., Leat, P.T. & Pankhurst, R.J. (eds). Terrane Processes at the Margins of Gondwana. *Geological Society, London, Special Publications* 246: 417-438.

Smellie, J. L., Martin, A.P., Panter, K.S., Kyle, P.R., & Geyer, A., 2020. Magmatism in Antarctica and its relation to Zealandia. *New Zealand Journal of Geology and Geophysics* 63: 578-588.

Storey, B. C., Leat, P.T., Weaver, S.D., Pankhurst, R.J., Bradshaw, J.D., & Kelley, S., 1999. Mantle plumes and Antarctica-New Zealand rifting: evidence from mid-Cretaceous mafic dykes. *Journal of the Geological Society* 156, 659–671.

Stracke, A., Hofmann, A.W., & Hart, S.R., 2005. FOZO, HIMU, and the rest of the mantle zoo. *Geochemistry, Geophysics, Geosystems.* DOI:10.1029/2004GC000824.

Streckeisen, A., 1976, To each plutonic rock its proper name. *Earth Science Reviews* 12, 1 – 33.

Suzuki, K., Senda, R., & Shimizu, K., 2011. Osmium behavior in a subduction system elucidated from chromian spinel in Bonin Island beach sands. *Geology* 39: 999–1002.

Taylor, W.R., 1998. An experimental test of some geothermometer and geobarometer formulations for upper mantle peridotites with application to the thermobarometry of fertile lherzolite and garnet websterite. *Neues Jahrbuch fur Mineralogie* 172: 381-408.

ten Brink, U.T., Hackney, R.I., Bannister, S., Stern T.A., & Makovsky, Y., 1997. Uplift of the Transantarctic Mountains and the bedrock beneath the East Antarctic ice sheet. *Journal of Geophysical Research* 102: 27,603-27,621.

Tulloch, A.J., Mortimer, N., Ireland, T.R., Waight, T.E., Maas, R., Palin, J.M., Sahoo, T., Seebeck, H., Sagar, M.W., Barrier, A., & Turnbull, R.E. 2019. Reconnaissance Basement Geology and Tectonics of South Zealandia. *Tectonics* 38: 516-551.

Upton, B.G.J., Downes, H., Kirstein, L.A., Bonadiman, C., Hill, P.G., & Ntaflos, T., 2011. The lithospheric mantle and lower crust-mantle relationships under Scotland: a xenolithic perspective. *Journal of the Geological Society, London* 168: 873-885.

Van der Wal, D., & Bodinier, J.-L., 1996. Origin of the recrystallisation front in the Ronda peridotite by km-scale pervasive porous melt flow. *Contributions to Mineralogy and Petrology* 122: 237-405.

van Wyk de Vries, M., Bingham, R. G., & Hein, A. S., 2017. A new volcanic province: an inventory of subglacial volcanoes in West Antarctica. *Geological Society of London, Special Publication* 461: 231–248.

Weaver, S.D., Adams, C.J., & Pankhurst, R.J., 1992. Granites of Edward VII Peninsula, Marie Byrd Land: anorogenic magmatism related to Antarctic-New Zealand rifting. *Transactions of the Royal Society of Edinburgh* 83: 281-290.

Weaver, S.D., Storey, B.C., Pankhurst, R.J., Mukasa, S.B., DiVenere, V.J., & Bradshaw, J.D., 1994. Antarctica-New Zealand rifting and Marie Byrd Land lithospheric magmatism linked to ridge subduction and mantle plume activity. *Geology* 22, 811–814.

Wells, T.R.A., 1977. Pyroxene thermometry in simple and complex systems. *Contributions to Mineralogy and Petrology* 62: 129-139.

Winberry, J.P., & Anandakrishnan, S., 2004. Crustal structure of the West Antarctic rift system and Marie Byrd Land hotspot. *Geology* 32: 977-980.

Wobbe, F., Gohl, K., Chambord, A., & Sutherland, R., 2012. Structure and breakup history of the rifted margin of West Antarctica in relation to Cretaceous separation from Zealandia and Bellingshausen plate motion. *Geochemistry, Geophysics, Geosystems* 13: 1-19. DOI:10.1029/2011GC003742.

Wysoczanski R.J., & Gamble J.A., 1992: Xenoliths from the volcanic province of West Antarctica and implications for lithospheric structure and processes. *In:* Yoshida, Y., Kaminuma, K., Shiraishi, K., (eds) Recent progress in Antarctic Earth Science, Terrapub, Tokyo, p273 - 277.

Wysoczanski, R.J., 1993. Lithospheric xenoliths from Marie Byrd Land volcanic province, West Antarctica. PhD Thesis, Victoria University of Wellington, 476pp.

Wysoczanski, R.J., Gamble, J.A., Kyle, P.R., & Thirlwall, M.F., 1995. The petrology of lower crustal xenoliths from the Executive Committee Range, Marie Byrd Land Volcanic Provnice, West Antarctica. *Lithos* 36: 185-201.

Yaxley, G.M., Crawford, A.J., & Green, D.H., 1991. Evidence for carbonatite metasomatism in spinel peridotite xenoliths from western Victoria, Australia. *Earth and Planetary Science Letters* 107: 305-317.

Figure captions

Fig. 1. (**a**) Outline map of Antarctica indicating area shown in b. (**b**) Map of West Antarctica showing Marie Byrd Land, with approximate boundaries of the West Antarctic Rift System (thick green dashed line) and Ross and Amundsen tectonostratigraphic provinces (green dotted line). The xenolith localities discussed in this paper are indicated by red-outlined polygons: FM, Fosdick Mountains; C, Mount Cumming and H, Mount Hampton, Executive Committee Range; A, Mount Aldaz, Usas Escarpment; M, Mount Murphy. Green dots indicate other Cenozoic volcanic centres within Marie Byrd Land; MF, Mountt Flint; MS, Mount Sidley. (**c**) Permian-Triassic reconstruction of Gondwana margin, after Elliot (2013): MBL, Marie Byrd Land; AP, Antarctic Peninsula; ChP, Challenger Plateau; CP, Campbell Plateau; CR, Chatham Rise; EM, Ellsworth Mountains; LHR, Lord Howe Rise; NZ E, eastern New Zealand; TI, Thurston Island. Grey regions indicate subaerial continental crust; green, subaqueous continental crust; blue, oceanic crust. Thick black line represents subduction plate boundary.

Fig. 2. Marie Byrd Land xenolith modal mineralogy on the ultramafic classification diagram (Streckeisen, 1976), by locality. Data from Cohen (2016) and this study. The majority of xenoliths fall within the lherzolite peridotite field, but include harzburgite, dunite, wehrlite and clinopyroxenite samples.

Fig. 3. Photomicrographs of representative xenoliths from Mount Cumming and Mount Hampton, Executive Committee Range, and Mount Aldaz, Usas Escarpment, showing textural and grain size variations. Textures are dominantly coarse granular (e.g. HAM1/69, Mt Hampton) but include well equilibrated, equigranular textures with 120° triple junctions (PK4A1, Mt Hampton) and samples exhibiting fine-grained deformation (90040C1, Mount Cumming). Exsolution lamellae are common in larger orthopyroxene grains (e.g. 90040E, Mount Cumming; MB69E, Mount Aldaz), and deformation bands in larger olivine grains (e.g. Ham1/69, Mount Hampton). MB69B, Mount Aldaz, contains a clinopyroxene-rich vein approximately 10 mm in diameter, with larger grains showing exsolution lamellae.

All imaged areas have the same field of view, approximately 4 mm, and are shown as both plane and cross polar light images. Ol, Olivine; Opx, orthopyroxene; Cpx, clinopyroxene; Spl, spinel.

Fig. 4. Selected mineral major element chemistry. (**a**) spinel Cr# versus olivine Mg#, with the Olivine - Spinel Mantle Array of Arai (1994) indicated by dashed grey lines. Data are from Chatzaras *et al*. (2016), predominantly from Fosdick Mountains localities. (**b**) and (**c**) Al_2O_3 and MgO in clinopyroxene (**b**) and orthopyroxene (**c**) from lherzolite and harzburgite samples. Green symbols, Mount Cumming; blue, Mount Hampton; orange, Mount Aldaz; red, Fosdick Mountains. Triangles represent samples from Chatzaras *et al*. (2016); circles and squares represent analyses of multiple grains from two xenoliths from each of Mounts Hampton, Cumming, and the Fosdick Mountains (this study; Supplementary file). Grey lines represent theoretical partial melting models from a primitive upper mantle source (McDonough and Sun, 1995) following Upton *et al*. (2011). Ticks represent 5% partial melting increments through to 25%.

Fig. 5. Chondrite normalised (Anders and Grevesse, 1989) REE diagrams for minerals from six xenoliths. Squares, clinopyroxene; diamonds, orthopyroxene; circles, olivine. Analyses of different grains from the same sample are indicated by different shading of symbols and lines.

Fig. 6. Primitive mantle normalised (McDonough and Sun, 1995) trace element diagrams for clinopyroxene from six xenoliths from Mounts Cumming and Hampton, Executive Committee Range (ECR), and Recess Nunatak and Demas Bluff, Fosdick Mountains. Four clinopyroxene are plotted for each sample, with analyses of different grains from the same sample indicated by different shading of symbols and lines. Data from individual samples typically closely overlap.

Fig. 7. Rare earth element partition coefficients (D) calculated for coexisting clinopyroxene and orthopyroxene. Thick lines represent calculated equilibrium partition coefficients at different temperatures for the xenolith compositions [(**a**) 940 and 1100°C (**b**) 940°C], following methods discussed in Liang *et al*. (2013). The H-MREE are in good agreement for all samples, with the LREE showing variable disequilibrium consistent with open system behaviour.

Fig. 8. Whole rock major element data (Wysoczanski, 1993). Grey crosses represent continental spinel peridotite xenoliths from off-cratonic regions in Australia, China, Japan, Europe, Siberia, North America, Algeria and Tanzania (see Supplementary file for full reference list). (**a**) – (**d**), curves represent calculated residual compositions from incremental batch melting of a MORB source at 2.0 GPa (dashed) and 1.5 GPa (solid) using the MELTS thermodynamic approach, after Aldanmaz *et al*. (2009).

Fig. 9. Strontium, Nd and Pb isotopes for Marie Byrd Land (MBL) peridotites. Inset in (a) shows sample with extreme Sr and Nd composition that plots outside of the area shown in (a). Grey crosses indicate pyroxenites from Executive Committee Range, Marie Byrd Land (Wysoczanski *et al*. 1995), and open diamonds are peridotites from southern Victoria Land (Martin *et al*. 2013). Fields for Marie Byrd Land crustal and mafic volcanic rocks and MORB (mid-ocean ridge basalts) from Wysoczanski *et al*. (1995); Panter *et al*. (2000) and; LeMasurier *et al*. (2016). NRHL, northern hemisphere reference line. BSE, bulk silicate earth; EMI, enriched mantle I; EMII, enriched mantle II and; HIMU, "high-μ" mantle endmember compositions (Stracke *et al*. 2005).

Fig. 10. Pressure-temperature diagram showing Marie Byrd Land peridotites, after Chatzaras *et al*. (2016). Temperatures are based on the Brey and Köhler (1990) thermometer and are plotted on a theoretical geotherm from Chatzaras *et al*. (2016; thick grey line). Also shown for comparison are the petrologic geotherm for McMurdo from Berg *et al*. (1989) and present-day Ross Embayment geotherm from ten Brink *et al*. (1997). Open red squares represent the calculated pressures of the spinel-garnet transition for each peridotite composition from Chatzaras *et al*. (2016), and provide a maximum pressure bound for those xenoliths used to constrain the theoretical geotherm.

Fig. 11. Primitive mantle normalised REE patterns for selected clinopyroxenes overlain with melt extraction models for spinel facies partial melting of a primitive upper mantle source for both batch (**a, c, e**) and fractional (**b, d, f**) melting. Patterns for different grains from the same sample are indicated by different shading of symbols. The degrees of melt extraction are indicated in panels (**a**) and (**b**), and were calculated using melting modes and partition coefficients from Johnston and Schwab (2004), Kelemen *et al*. (1993) and references therein. Purple overlay in panel (**b**), shows field of clinopyroxene that underwent melting in garnet facies prior to re-equilibrating in spinel facies from Bonadiman *et al*. (2005). Primitive mantle composition from McDonough and Sun (1995).

Table 1. *Xenolith localities and references*

Volcanic Centre	Latitude (S)	Longitude (W)	Reference/Source
Executive Committee Range			
Mount Cumming	76.667	125.820	*Wysoczanski 1993; Handler et al. 2003; Cohen 2016; Chatzaras et al. 2016*
Mount Hampton	76.48	125.97	*Wysoczanski 1993; Handler et al. 2003; Moreira & Madureira, 2005*
USAS Escarpment			
Mount Aldaz	76.051	124.417	*Wysoczanski 1993; Handler et al. 2003; Cohen 2016; Chatzaras et al. 2016*
Fosdick Mountains			
Mount Avers	76.481	145.396	*Cohen 2016; Chatzaras et al. 2016*
Bird Bluff	76.504	144.598	*Cohen 2016; Chatzaras et al. 2016*
Demas Bluff	76.568	144.853	*Cohen 2016; Chatzaras et al. 2016*
Marujupu	76.508	145.670	*Cohen 2016; Chatzaras et al. 2016*
Recess Nunatak	76.519	144.507	*Cohen 2016; Chatzaras et al. 2016*
Walgreen Coast			
Mount Murphy	75.33	110.51	*Wysoczanski 1993*

Table 2. *Selected mineral compositions.*

	Mount Cumming		Mount Hampton		Demas Bluff		W Recess Nunatak
	MC1999	2000/2	PK91005	2000/12	2000/8	1998/99	1998
Olivine							
SiO_2 (wt%)	41.67	41.34	41.40	43.07	41.21	42.09	41.94
TiO_2	0.06	0.02	0.06	0.05	0.05	0.06	0.17
Al_2O_3	0.05	0.02	0.06	0.05	0.04	0.02	0.04
FeO	9.46	8.44	8.38	8.93	8.86	9.01	8.68
MnO	0.18	0.10	0.21	0.12	0.13	0.18	0.19
MgO	49.16	49.85	49.97	49.55	48.94	50.30	49.95
CaO	0.11	0.07	0.11	0.12	0.05	0.05	0.12
Na_2O	0.02	0.01	0.09	0.04	0.05	0.02	0.05
K_2O	0.02	0.03	0.04	0.03	0.00	0.11	0.10
Cl	0.03		0.03		0.01	0.07	0.09
Cr_2O_3	0.11	0.04	0.04	0.09	0.04	0.12	0.06
NiO	0.37	0.10	0.40	0.12	0.08	0.41	0.44
Total	101.23	100.04	100.79	102.14	99.43	102.44	101.83
Mg#	90.3	91.3	91.2	90.8	90.8	90.9	91.2
Orthopyroxene							
SiO_2 (wt%)	55.13	56.31	55.97	56.40	55.12	56.48	56.81
TiO_2	0.33	0.07	0.09	0.13	0.12	0.18	0.27
Al_2O_3	3.93	3.38	3.23	3.80	3.77	3.99	3.62
FeO	6.11	5.37	5.30	5.68	5.33	5.62	5.62
MnO	0.17	0.13	0.17	0.15	0.13	0.20	0.14
MgO	32.97	33.94	33.61	32.60	32.68	33.99	33.70
CaO	0.99	0.68	0.99	0.98	1.22	0.63	0.61
Na_2O	0.07	0.06	0.11	0.12	0.15	0.11	0.12
K_2O	0.05	0.02	0.07	0.02	0.04	0.03	0.14
Cl	0.05		0.04			0.06	0.13
Cr_2O_3		0.69	0.77	0.67		0.56	0.60
NiO		0.09	0.15	0.06		0.15	0.17
Total	99.79	100.74	100.49	100.60	98.56	102.01	101.94
Mg#	90.6	91.8	91.9	91.1	91.6	91.5	91.4
Mg	88.85	90.65	90.12	89.33	89.39	90.42	90.37
Fe	9.23	8.05	7.97	8.73	8.18	8.39	8.46
Ca	1.92	1.30	1.91	1.94	2.43	1.20	1.17
Clinopyroxene							
SiO_2 (wt%)	50.44	53.00	52.61	52.82	52.50	52.67	53.04
TiO_2	1.01	0.21	0.05	0.26	0.43	0.53	0.48
Al_2O_3	5.68	4.17	3.63	4.70	5.71	6.31	5.55
FeO	3.29	2.04	2.44	2.61	2.29	2.70	2.30
MnO	0.18	0.10	0.14	0.13	0.11	0.15	0.12
MgO	16.32	16.82	17.52	16.72	15.08	15.01	15.17
CaO	20.65	21.87	21.08	20.56	20.24	21.14	21.14
Na_2O	0.83	1.00	0.72	1.10	1.97	1.80	2.00
K_2O	0.04	0.01	0.04	0.03	0.03	0.04	0.16
Cl	0.04		0.04		0.03	0.05	0.12
Cr_2O_3		1.20	1.15	1.40	1.64	1.10	1.55
NiO		0.06	0.13	0.06	0.05	0.08	0.12
Total	98.47	100.46	99.55	100.39	99.85	101.58	101.74
Mg#	89.9	93.6	92.8	91.9	92.1	90.8	92.2
Mg	49.44	49.93	51.46	50.71	48.77	47.32	47.93
Fe	5.58	3.40	4.01	4.45	4.16	4.77	4.08
Ca	44.98	46.68	44.52	44.83	47.07	47.90	48.00

Table 3. *Sr, Nd, Pb and Os isotopic data*

sample	Al_2O_3 (wt%)	CaO (wt%)	Sr (ppm)	$^{87}Sr/^{86}Sr$	Nd (ppm)	Sm (ppm)	εNd	$^{143}Nd/^{144}Nd$	$^{147}Sm/^{144}Nd$	T_{DM} (Ma)	$^{206}Pb/^{204}Pb$	$^{207}Pb/^{204}Pb$	$^{208}Pb/^{204}Pb$	Re (ppb)	Os (ppb)	$^{187}Re/^{188}Os$	$^{187}Os/^{188}Os$	γOs	T_{RD} (Ma)	T_{MA} (Ma)
Executive Committee Range																				
Mount Hampton																				
PK1A	1.90	1.62	11.5	0.70284(3)	0.784	0.230	1.3	0.51275(1)	0.177	1,861	19.5(6)	15.38(4)	38.50(12)	0.074	0.88	0.0783(8)	0.11907(9)	-7.5	1,347	1,648
PK4H	0.62	0.54	2	0.70307(4)	0.166	0.275	5.1	0.51294(4)	1.000	-48	17.85(5)	15.21(4)	35.9(3.5)	0.001	2.42	0.0011(1)	0.12064(9)	-6.3	1,130	1,132
PK4Z	1.15	0.91	2	0.70365(4)	0.031	0.010					19.12(1)	15.60(1)	38.69(2)	0.005	2.81	0.0122(1)	0.1214(2)	-5.7	1,025	1,055
PK4J1	2.33	1.58	3.2	0.70267(3)	0.291	0.096	8.2	0.51310(2)	0.200	1,009	18.88(4)	15.33(4)	38.18(10)	0.061	1.41	0.206(2)	0.1214(1)	-5.7	1,021	1,966
														0.044	1.48	0.1483(15)	0.12151(9)	-5.6	1,009	1,544
PK4P1	4.07	3.17	4	0.70248(3)	0.454	0.251	9.9	0.51319(1)	0.334	-8	19.071(6)	15.566(5)	38.55(1)	0.174	2.49	0.337(3)	0.12768(7)	-0.8	144	694
PK5C	0.84	0.39	7	0.70309(3)							19.47(1)	15.52(1)	39.09(8)	0.256	2.13	0.584(6)	0.12809(7)	-0.5	86	-
					0.413	0.152	7.2	0.51305(1)	0.223	-	19.28(1)	15.55(1)	38.56(2)	0.350	2.24	0.529(5)	0.12823(8)	-0.4	66	-
PK5I	2.09	1.09									19.641(4)	15.636(4)	39.18(1)	0.000	0.88	0.0000	0.1219(1)	-5.3	953	953
PK5M	0.85	0.64	2	0.70349(3)										0.004	1.56	0.0119(1)	0.12064(9)	-6.3	1,130	1,162
PK4O	3.26	2.95												0.109	0.61	0.867(9)	0.1258(2)	-2.2	407	-
Mount Cumming																				
90040E	3.59	3.10	12	0.70279(4)		0.274	1.3	0.51270(2)	0.190	3,142	19.104(6)	15.569(5)	38.2(4)	0.031	0.39	0.378(4)	0.1288(3)	0.1	-	-
90040M														0.044	0.82	0.261(3)	0.1272(2)	-1.2	215	555
90040K	1.62	1.57	8	0.70302(3)	0.308	0.066	4.5	0.51287(2)	0.130	592	19.561(3)	15.636(2)	38.69(1)	0.001	14.4	0.0004(1)	0.12263(5)	-4.7	853	853
											19.258(6)	15.648(5)	38.88(1)							
MC 1					0.577	0.179	5.9	0.51294(2)	0.187	1,460	18.718(8)	15.552(6)	38.30(2)	0.045	2.95	0.0724(7)	0.11794(8)	-8.4	1,503	1,808
USAS Escarpment																				
Mount Aldaz																				
MB69A	3.68	3.29									19.201(8)	15.590(6)	38.73(2)	0.221	3.27	0.338(3)	0.12778(8)	-0.7	130	639
MB69E	3.24	3.08	3.0	0.70191(3)	0.209	0.141	22.9	0.51381(2)	0.407	488	18.34(1)	15.29(2)	37.34(5)	0.184	3.69	0.243(2)	0.12576(7)	-2.3	414	964
MB69F	3.36	3.38	6	0.70298(2)	0.382	0.146	6.1	0.51295(1)	0.318	-	19.172(4)	15.626(3)	38.564(8)	0.176	1.46	0.583(6)	0.1318(1)	2.4	-	1,165
				0.70295(4)										0.077	1.51	0.246(3)	0.1333(2)	3.5	-	-
MB69H	2.76	2.47	10	0.70277(3)	0.350	0.165	8.9	0.51309(1)	0.285	-	18.611(4)	15.589	38.06(1)	0.101	3.19	0.152(2)	0.12466(9)	-3.1	569	885
											18.597(2)	15.571	37.987(4)							
Fosdick Mountains																				
Western Recesses															2.50		0.11623(8)	-9.7	1,739	-
Demas Bluff														0.038	3.09	0.0538(5)	0.1222(1)	-5.0	911	1,042

Table 4. *Temperature estimates from two-pyroxene geothemometers*

Locality/Sample	Major elements in pyroxene			REE in pyroxene
	Wells (1977) (°C)	B&K'90* (°C)	Putirka (2008) (°C)	Liang et al. (2013) (°C)
West Recess Nunatak	846	808	950	965±105
Demas Bluff				
2000/8	908	876	959	926±14
2000/3		930	1009	
Mount Hampton				
2000/12	1008	1048	1070	1088±22
PK 91005	1023	1038	1065	1108±16
Mount Cumming				
2000/2	965	929	992	957±22
WA/4	973	1025	1006	

*B&K '90; Brey and Köhler (1990), calculated assuming a pressure of 1.5GPa

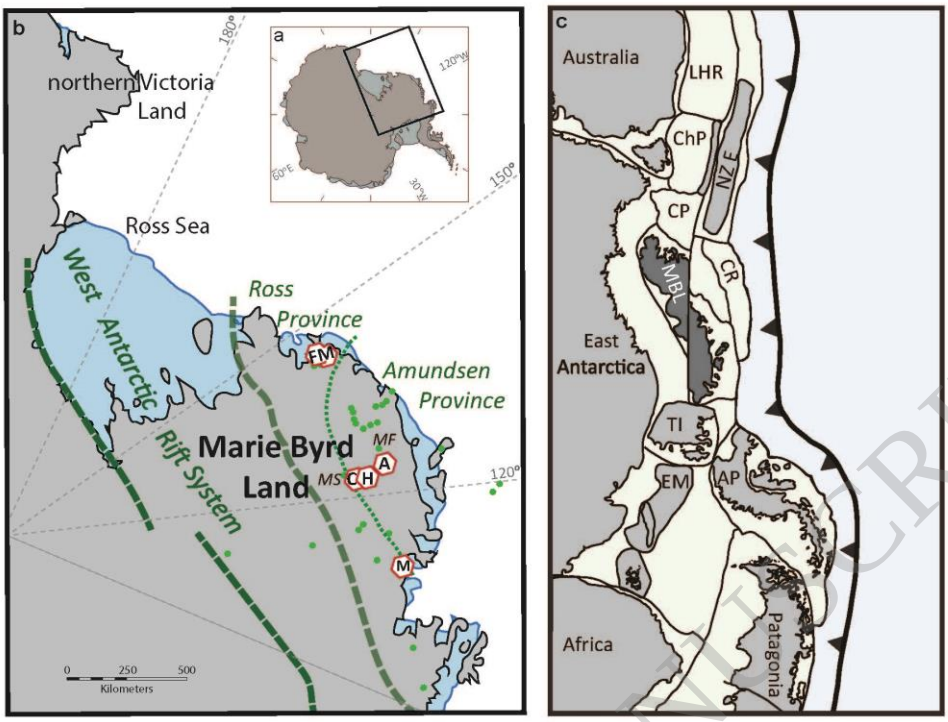

Figure 1

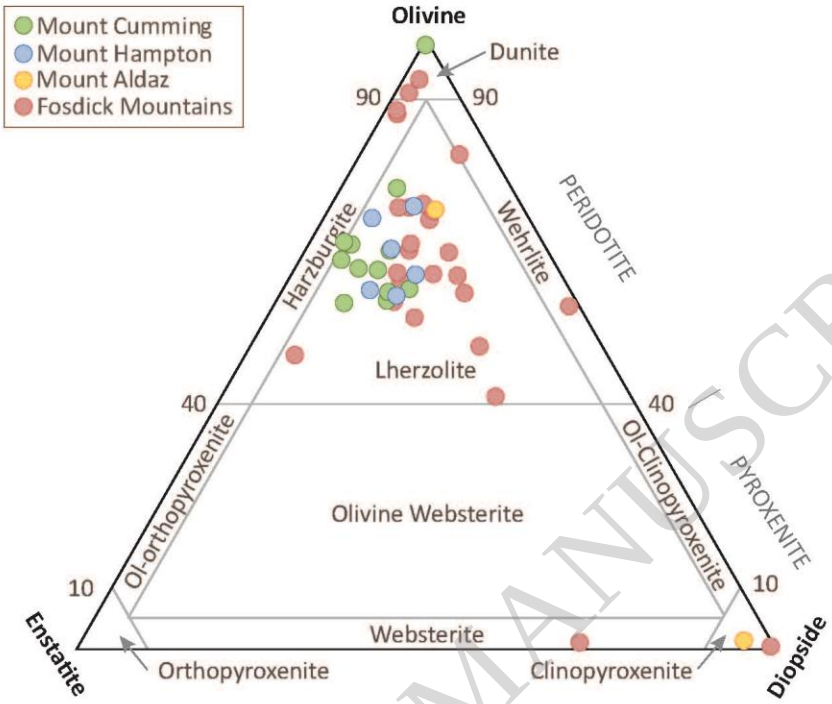

Figure 2

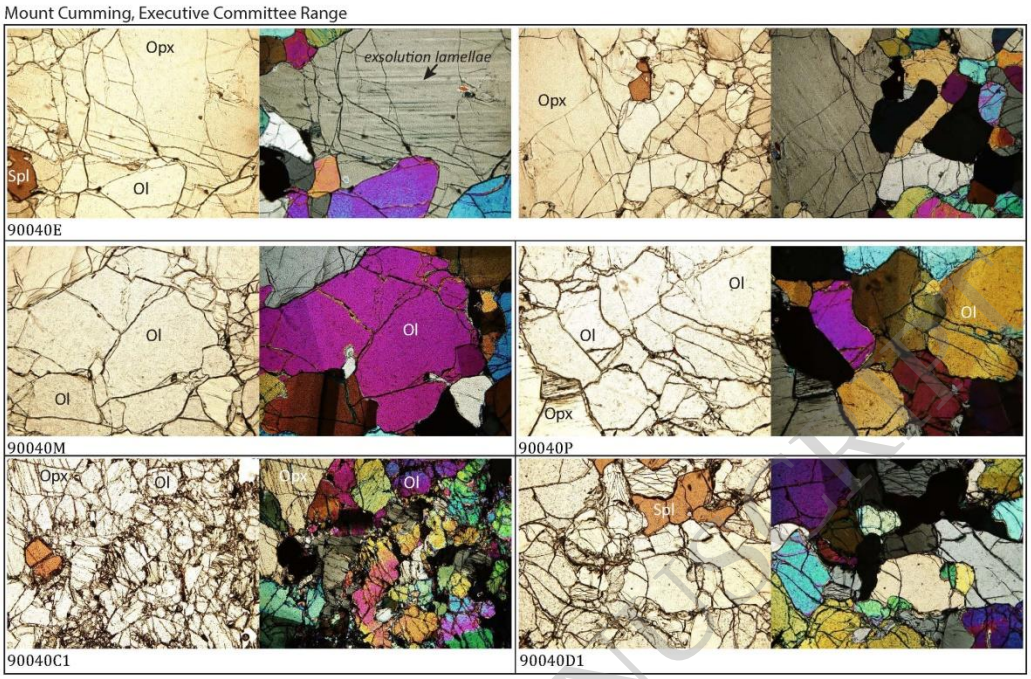

Figure 3

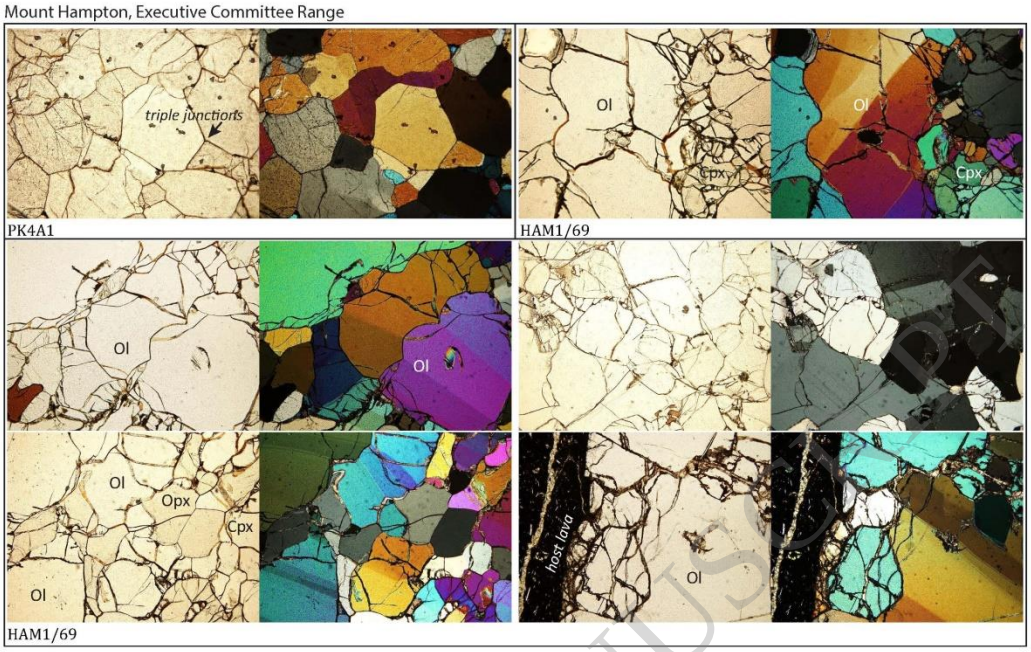

Figure 3 cont.

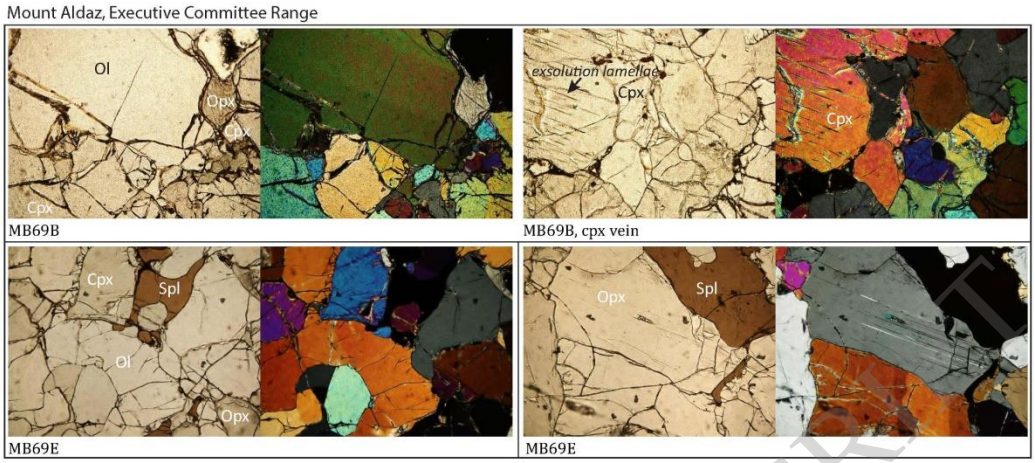

Figure 3 cont.

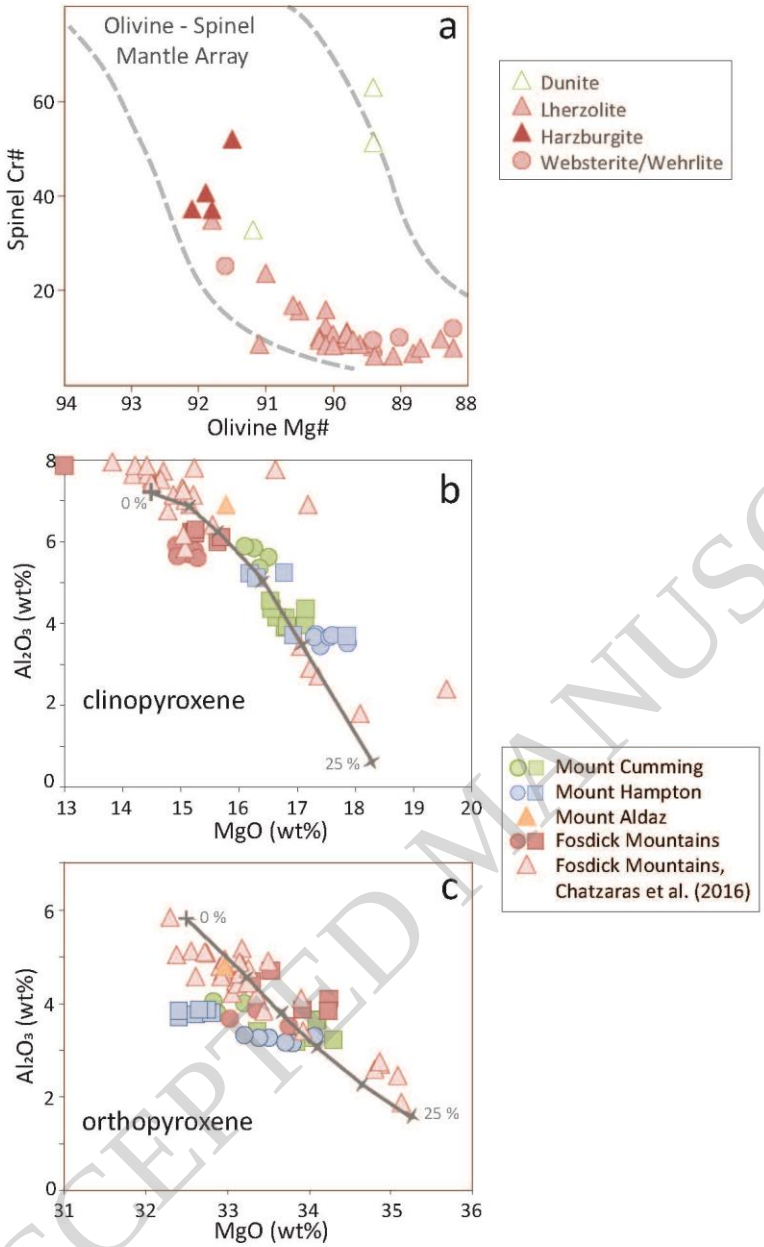

Figure 4

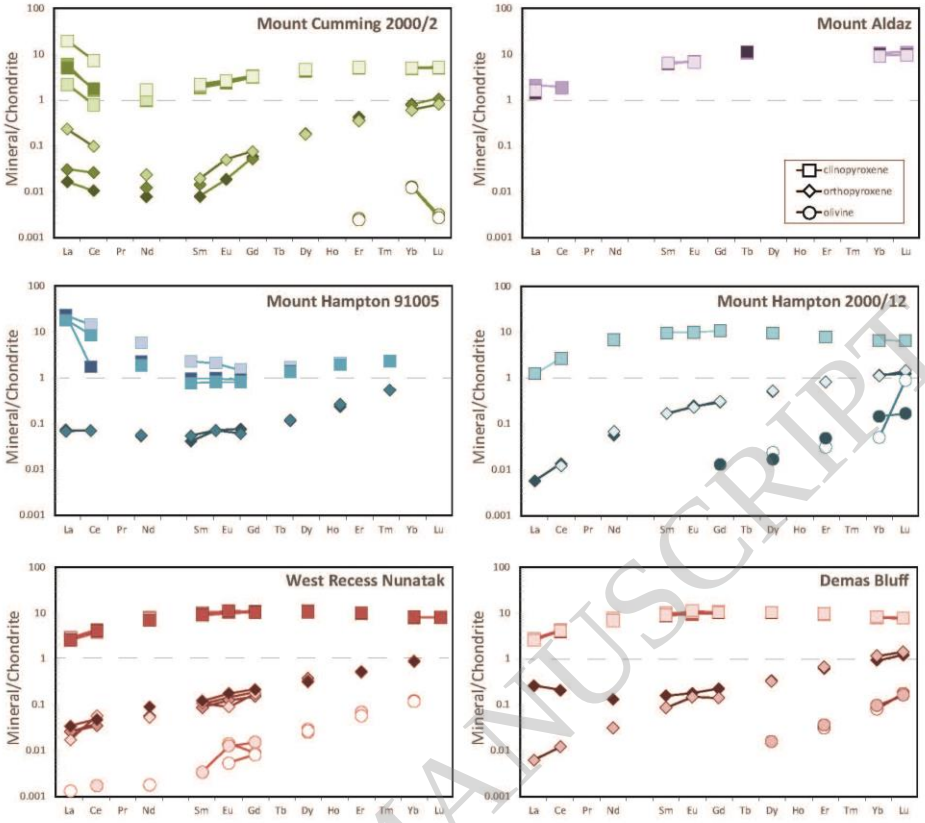

Figure 5

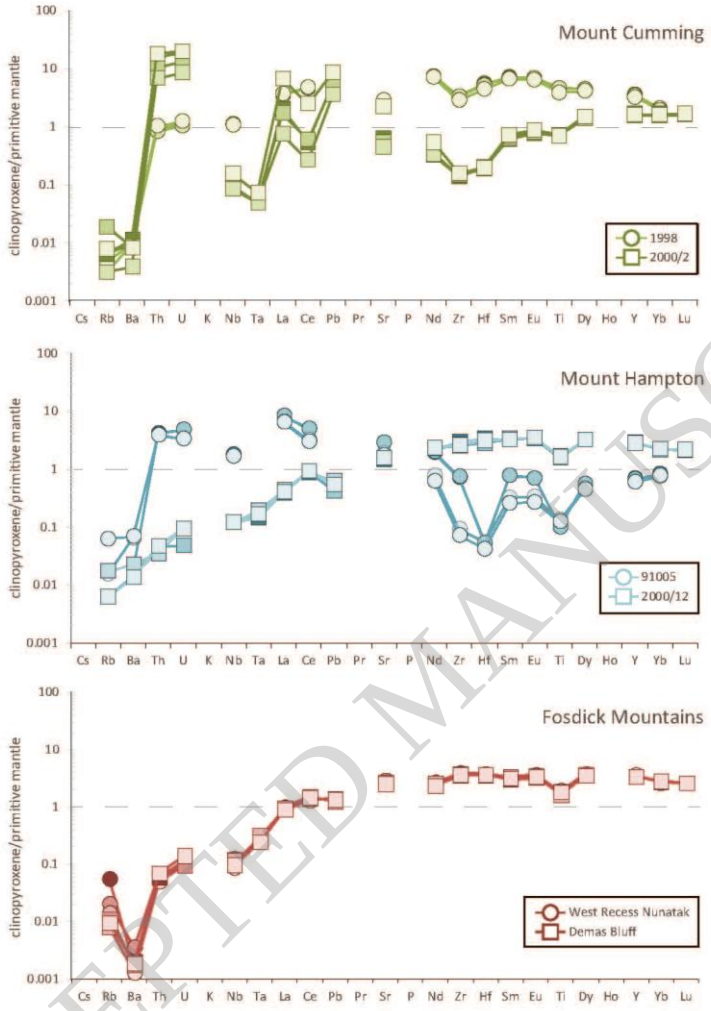

Figure 6

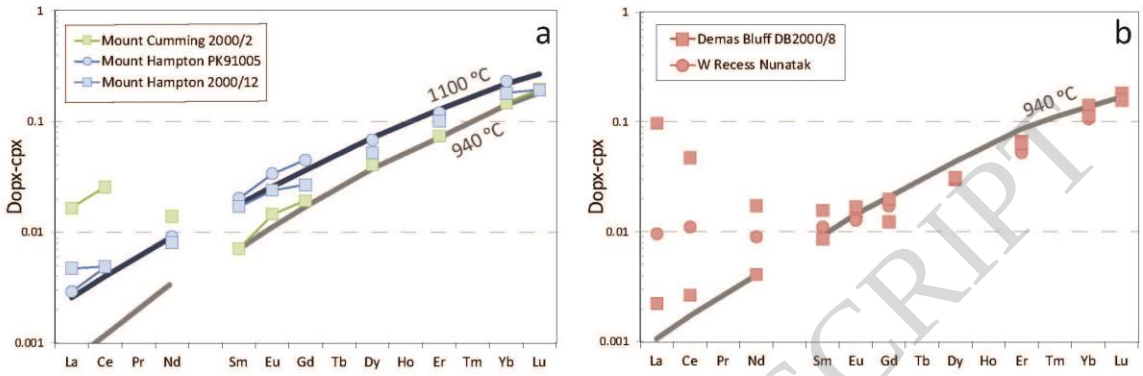

Figure 7

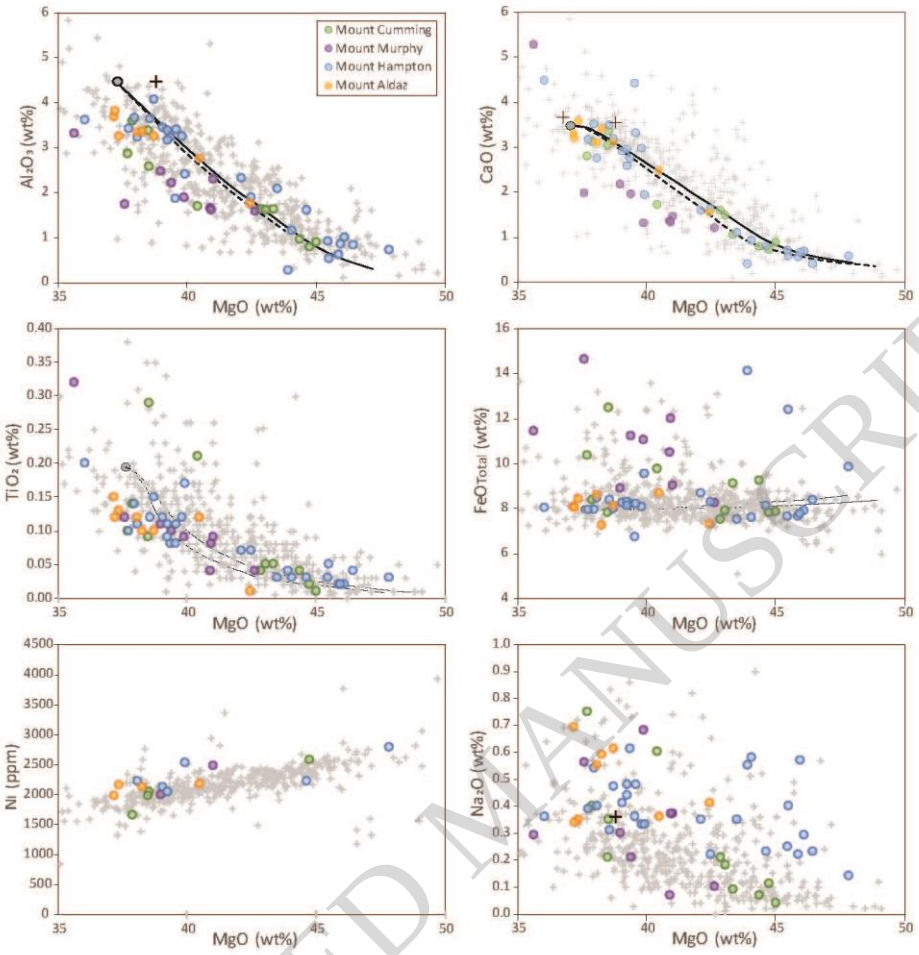

Figure 8

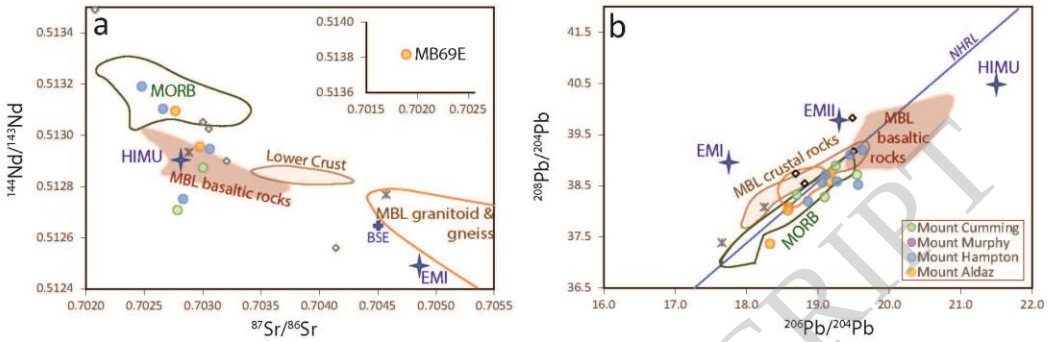

Figure 9

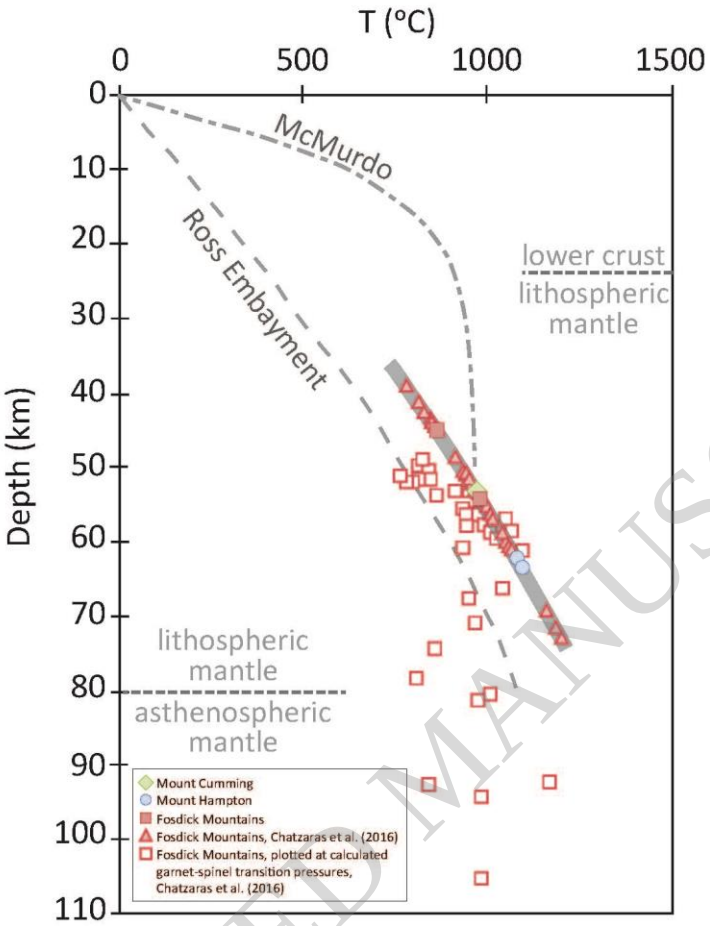

Figure 10

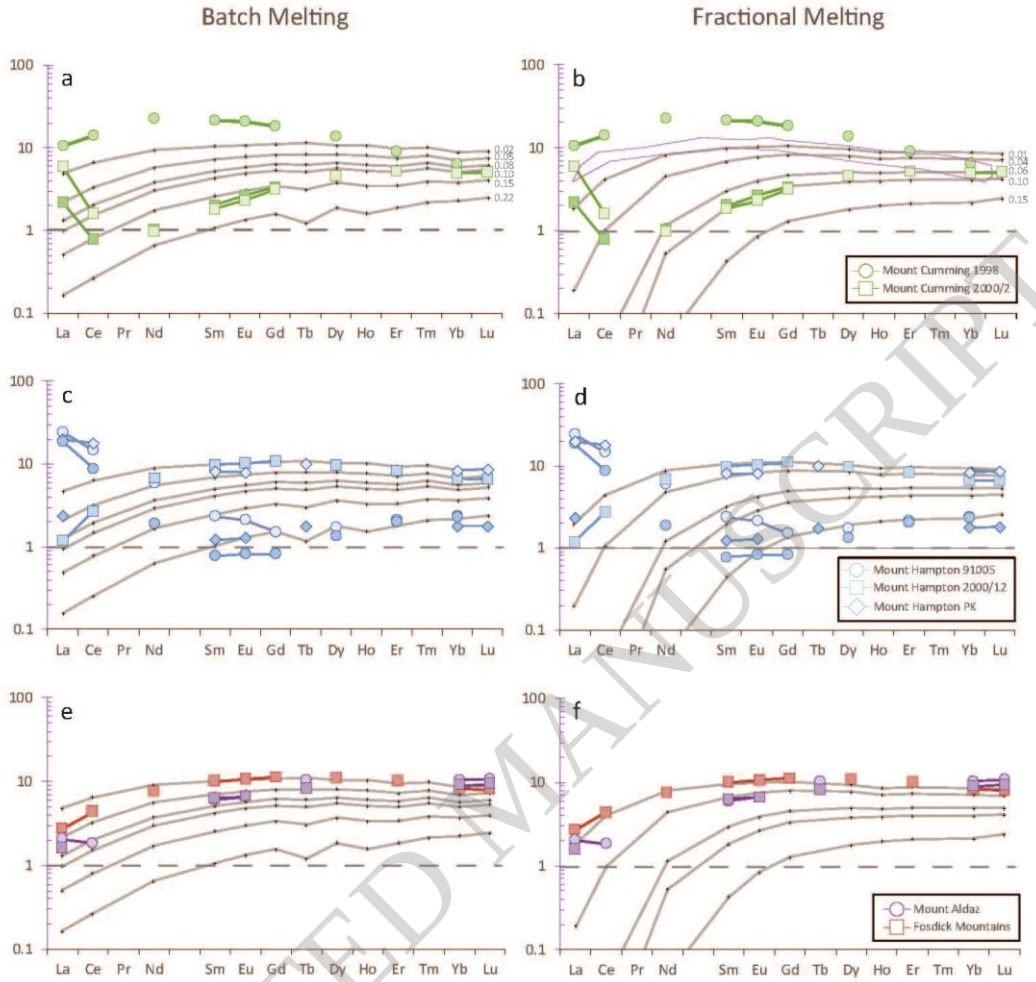

Figure 11